XXXI Symposium on Bioinformatics and Computer-Aided Drug Discovery (BCADD-2025)

# An Integrated Computational Strategy for Profiling Terpenoid for Dual-target leads against *Klebsiella pneumoniae* penicillin-binding protein 3 (PBP3) and Beta-lactamase

***Gideon Ampoma Gyebi and Saheed Sabiu***

*Department of Biotechnology and Food Science, Faculty of Applied Sciences, Durban University of Technology, P.O. Box 1334, Durban 4000, South Africa*


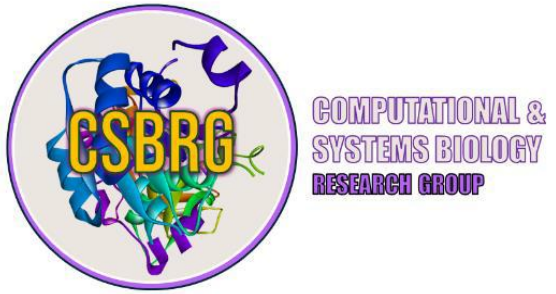

# Introduction

***Antibiotic resistance***

Terpenoid scaffold

**Penicillin-binding protein 3 (PBP3)**

**β-lactamases**

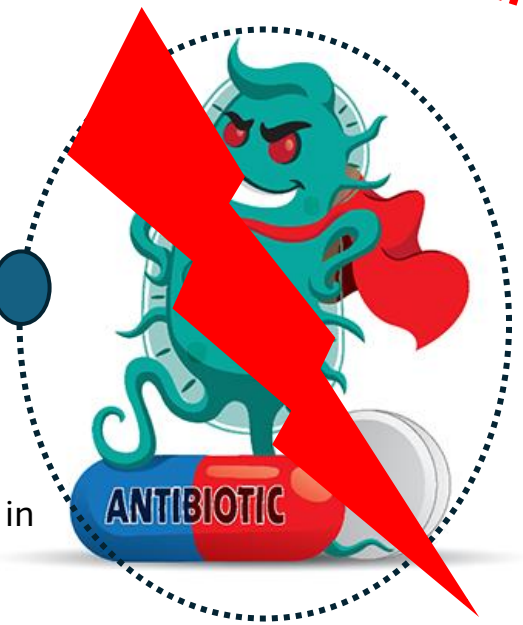


Mechanism of drug resistance in ***Klebsiella pneumoniae***

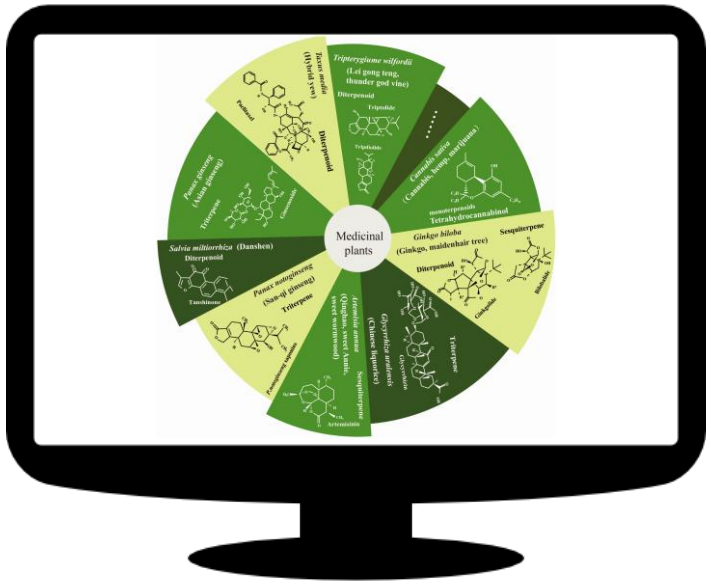


Integrated computational methods

**Aim:** identify leads terpenoid for dual-target against *K. pneumoniae* PBP3 & Beta-lactamase

ESKAPE pathogens

COMPUTATIONAL & SYSTEMS BIOLOGY RESEARCH GROUP

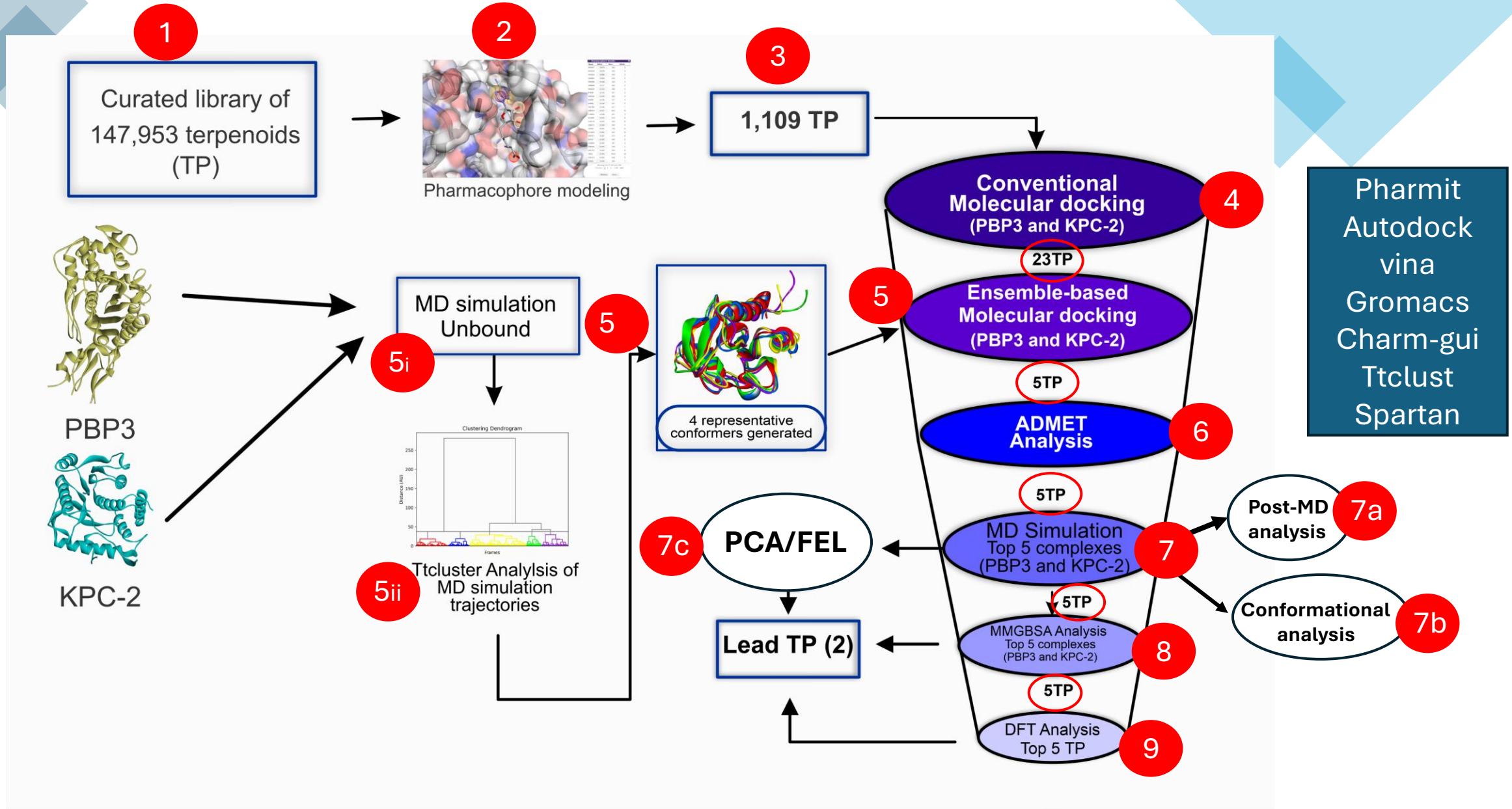


**Figure 2:** *Workflow diagram of the study*

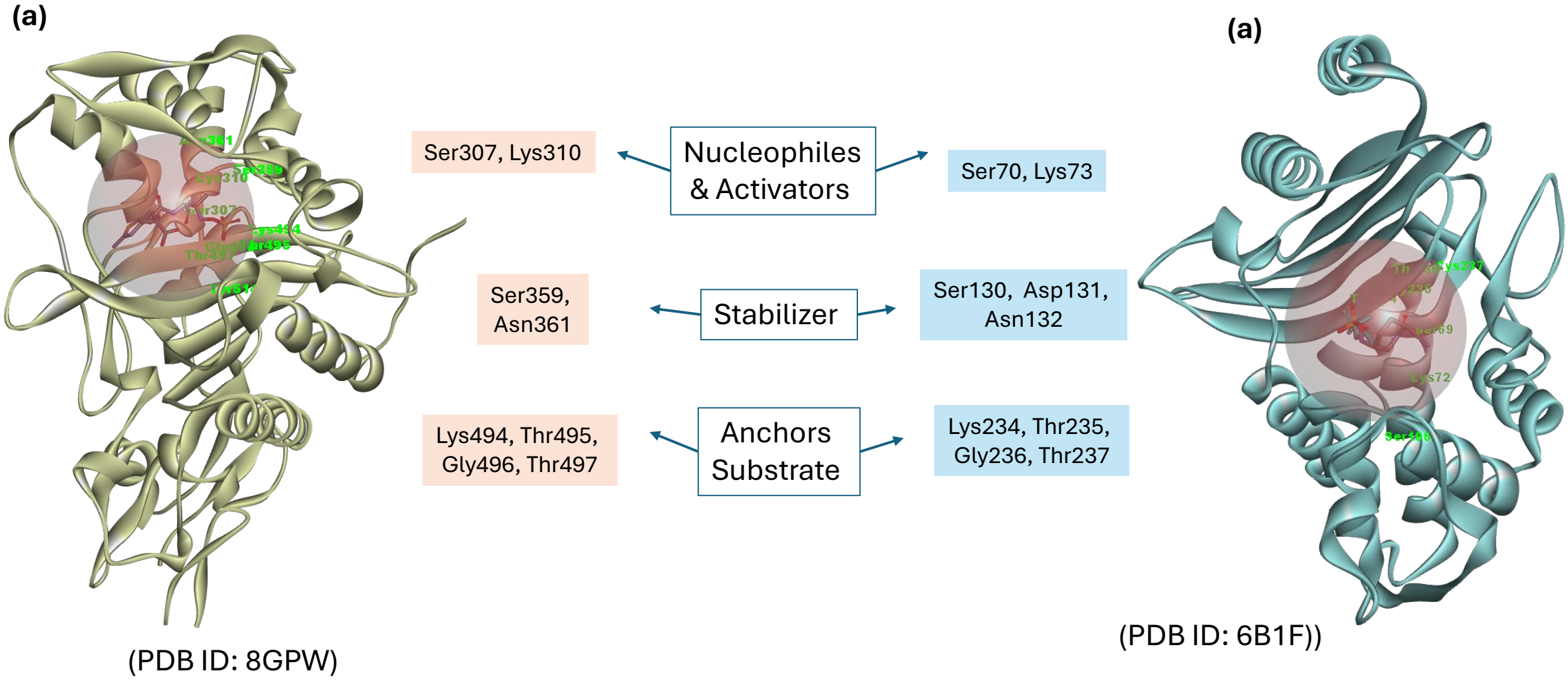


Cartoon representation of showing binding site residues of (a) *Klebsiella pneumoniae* PBP3 and (b) Beta-lactamase

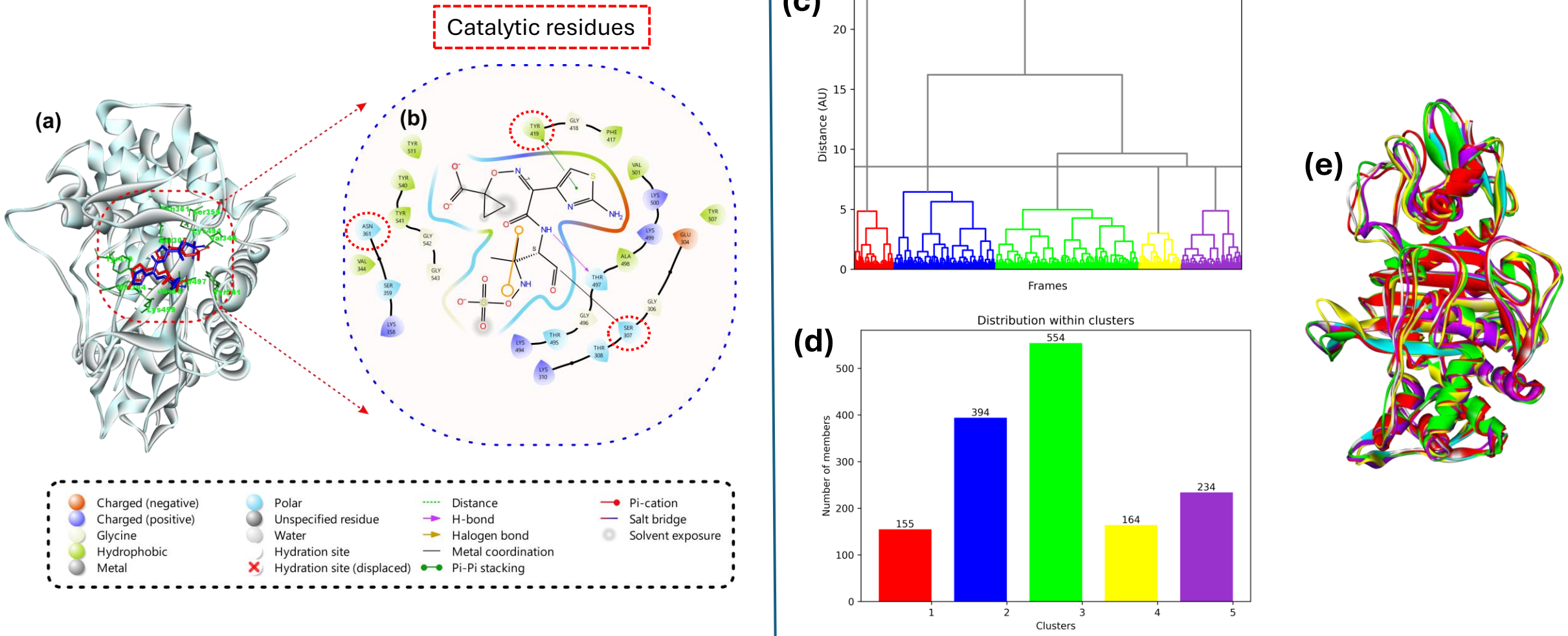


**Figure 3 (a)** The best-docked conformer of ligand 18G (red) superimposed on the native ligand (blue) in the *K. pneumoniae* PBP3 active site to validate the molecular docking protocol. The computed RMSD (1.37 Å) using Discovery Studio Visualiser version 20 (https://discover.3ds.com/) shows the replicated docking conformation; **(b)** amino acid plots of docked ligand 18G showing interacting residue; **(c)** clustering dendrogram showing the arrangement of clusters; **(d)** frames distribution within the clusters and **(e)** superimposed conformations (5) generated from the ttcluster analysis of trajectories generated from the MD simulation of unbound *K. pneumoniae* PBP3

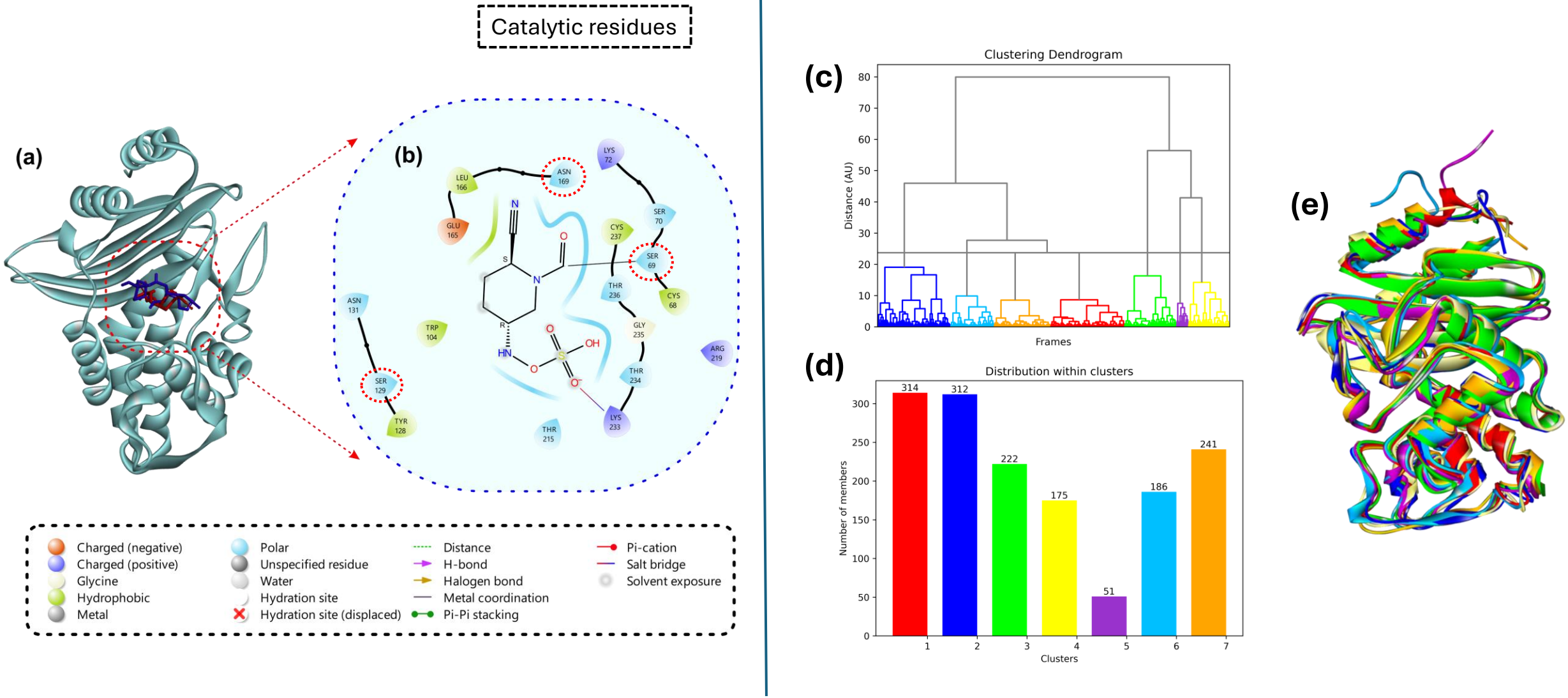


**Figure 4: (a)** The best-docked conformer of ligand 18G (red) superimposed on the native ligand (blue) in the *K. pneumoniae* PBP3 active site to validate the molecular docking protocol. The computed RMSD (1.39 Å) using Discovery Studio Visualiser version 20 (https://discover.3ds.com/) shows the replicated docking conformation; **(b)** amino acid plots of docked ligand 18G showing interacting residue; **(c)** clustering dendrogram showing the arrangement of clusters; **(d)** frames distribution within the clusters and **(e)** superimposed conformations (5) generated from the ttcluster analysis of trajectories generated from the MD simulation of unbound *K. pneumoniae* KPC-2 β-lactamase

| S/no | Compounds | Binding scores (kcal/mol) | |
|---|---|---|---|
| | | PBP3 | KPC-2 |
| | | CD | CD |
| S1 | 18G | –7.4 | |
| S2 | Ceftaroline | –8.3 | |
| S3 | WCK 4234 | | –7.6 |
| S4 | Clavulanate | | –6.2 |
| 1 | TP77265 | –10.5 | –9.5 |
| 2 | TP156670 | –10.4 | –8.9 |
| 3 | TP71512 | –10.4 | –9.3 |
| 4 | TP102455 | –10.4 | –8.6 |
| 5 | TP115627 | –10.2 | –8.6 |
| 6 | TP124709 | –10.2 | –9.4 |
| 7 | TP37236 | –10.2 | –10.2 |
| 8 | TP34359 | –10.2 | –8.8 |
| 9 | TP74139 | –10.1 | –9.3 |
| 10 | TP85431 | –10.1 | –9 |
| 11 | TP127968 | –10.1 | –9.1 |
| 12 | TP151931 | –10.1 | –8.1 |
| 13 | TP93780 | –10.1 | –8.9 |
| 14 | TP64159 | –10 | –10.2 |
| 15 | TP70837 | –10 | –8.1 |
| 16 | TP94518 | –10 | –8.7 |
| 17 | TP96783 | –10 | –9 |
| 18 | TP99879 | –10 | –7.1 |
| 19 | TP100288 | –10 | –8.5 |
| 20 | TP138571 | –10 | –8.3 |
| 21 | TP183163 | –10 | –8.3 |
| 22 | TP183349 | –10 | –8.2 |
| 23 | TP555 | –10 | –8.0 |

**Table 1:** Docking scores of top ranked terpenoids and reference standard against targets

***Notes***
***TP:*** *Terpenoid ID*
***CD:*** *Conventional docking;*
***EB D****: Ensemble-based Docking*
*presented as mean ± SD*
*of the binding scores to the conformers*

| S/no | Compounds | Binding scores (kcal/mol) | | | |
|---|---|---|---|---|---|
| | | PBP3 | | KPC-2 | |
| | | CD | EBD | CD | EBD |
| **S1** | 18G | –7.4 | –6.58 ± 1.1 | | |
| **S2** | Ceftaroline | –8.3 | –7.22 ± 1.1 | | |
| **S3** | WCK 4234 | | | –7.6 | –6.9 ± 1.1 |
| **S4** | Clavulanate | | | –6.2 | –6.2 ± 0.9 |
| **1** | **TP77265** | **–10.5** | **–8.81 ± 0.8** | **–9.5** | **–8.91 ± 0.8** |
| **2** | **TP156670** | **–10.4** | **–8.95 ± 1.2** | **–8.9** | **–8.61 ± 0.8** |
| **3** | TP71512 | –10.4 | –8.12 ± 1.2 | –9.3 | –8.82 ± 1.1 |
| **4** | TP102455 | –10.4 | –8.12 ± 0.9 | –8.6 | –7.82 ± 0.7 |
| **5** | TP115627 | –10.2 | –8.25 ± 0.9 | –8.6 | –8.81 ± 1.2 |
| **6** | **TP124709** | **–10.2** | **–9.07 ± 1.0** | **–9.4** | **–8.8 ± 0.9** |
| **7** | TP37236 | –10.2 | –8.05 ± 0.9 | –10.2 | –8.15 ± 0.8 |
| **8** | TP34359 | –10.2 | –8.08 ± 1.5 | –8.8 | –8.41 ± 1.0 |
| **9** | TP74139 | –10.1 | –8.18 ± 1.3 | –9.3 | –8.28 ± 1.0 |
| **10** | TP85431 | –10.1 | –8.24 ± 0.9 | –9 | –8.59 ± 0.7 |
| **11** | TP127968 | –10.1 | –7.81 ± 1.2 | –9.1 | –8.22 ± 0.8 |
| **12** | TP151931 | –10.1 | –7.61 ± 0.8 | –8.1 | –7.29 ± 0.8 |
| **13** | TP93780 | **–10.1** | **–8.81 ± 0.7** | **–8.9** | **–8.21 ± 0.7** |
| **14** | TP64159 | **–10** | **–8.85 ± 0.9** | **–10.2** | **–9.15 ± 0.9** |
| **15** | TP70837 | –10 | –8.15 ± 0.9 | –8.1 | –7.82 ± 0.9 |
| **16** | TP94518 | –10 | –8.29 ± 1.1 | –8.7 | –8.22 ± 0.9 |
| **17** | TP96783 | –10 | –8.27 ± 1.2 | –9 | –8.31 ± 1.5 |
| **18** | TP99879 | –10 | –8.57 ± 1.1 | –7.1 | –7.32 ± 0.7 |
| **19** | TP100288 | –10 | –7.86 ± 1.8 | –8.5 | –8.21 ± 0.9 |
| **20** | TP138571 | –10 | –8.24 ± 1.2 | –8.3 | –7.84 ± 1.1 |
| **21** | TP183163 | –10 | –8.14 ± 1.2 | –8.3 | –7.54 ± 1.1 |
| **22** | TP183349 | –10 | –7.91 ± 0.9 | –8.2 | –7.79 ± 0.8 |
| **23** | TP555 | –10 | –8.18 ± 1.3 | –8.0 | –7.81 ± 1.0 |

**Table 1:** Docking scores of top ranked terpenoids and reference standard against targets

***Notes***
***TPID:*** *Terpenoid ID*
***CD:*** *Conventional docking;*
***EB D****: Ensemble-based Docking*
*presented as mean ± SD*
*of the binding scores to the conformers*

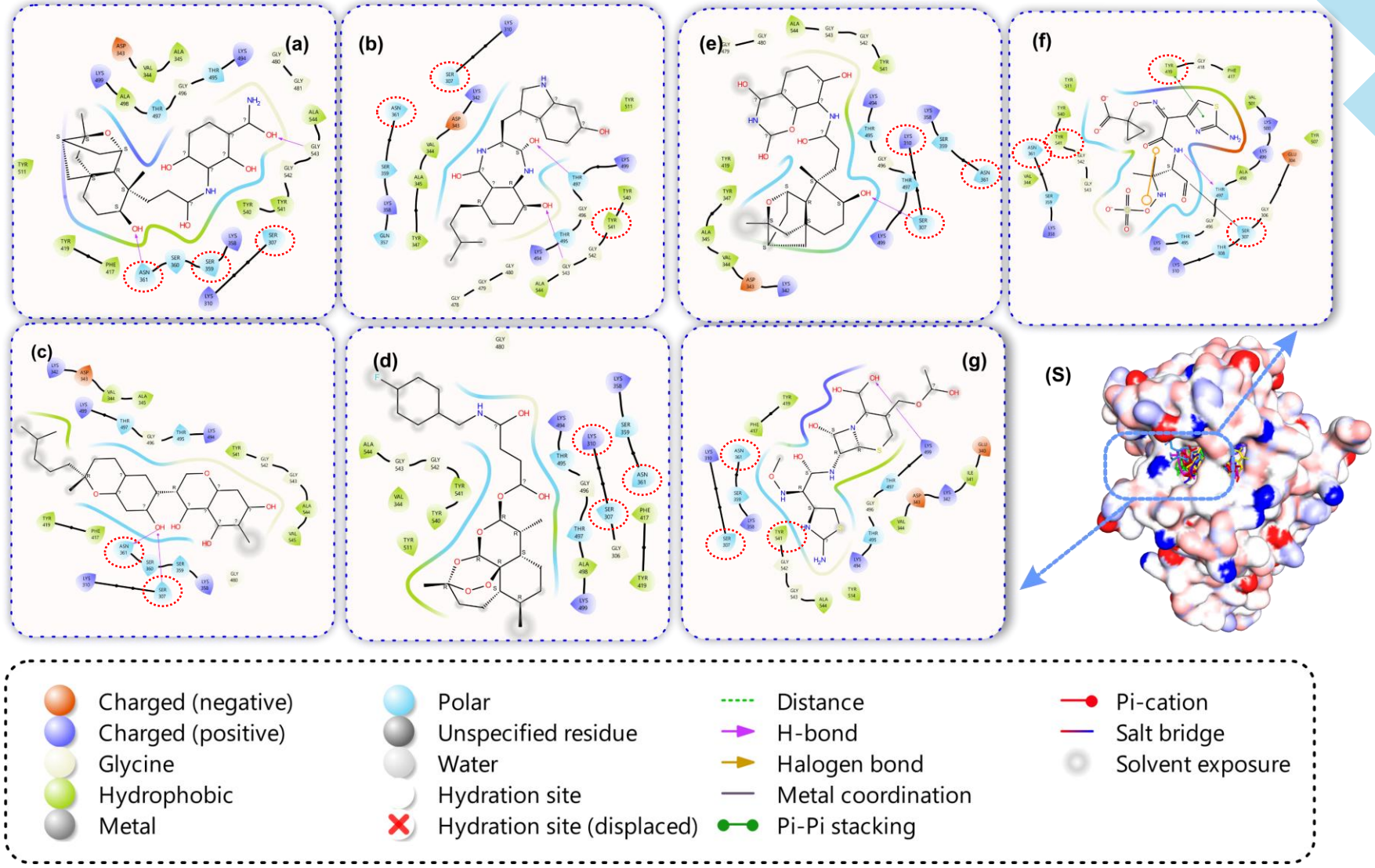


**Figure 6:** Amino acid interactive plots of top-ranked terpenoids and reference inhibitor (ceftaroline) in the active site of *K. pneumoniae* PBP3. The ligands are displayed as sticks (a) TP64159; (b) TP77265; (c) TP93780; (d) TP124709; (e) TP156670; (f) 18G and (g) ceftaroline.

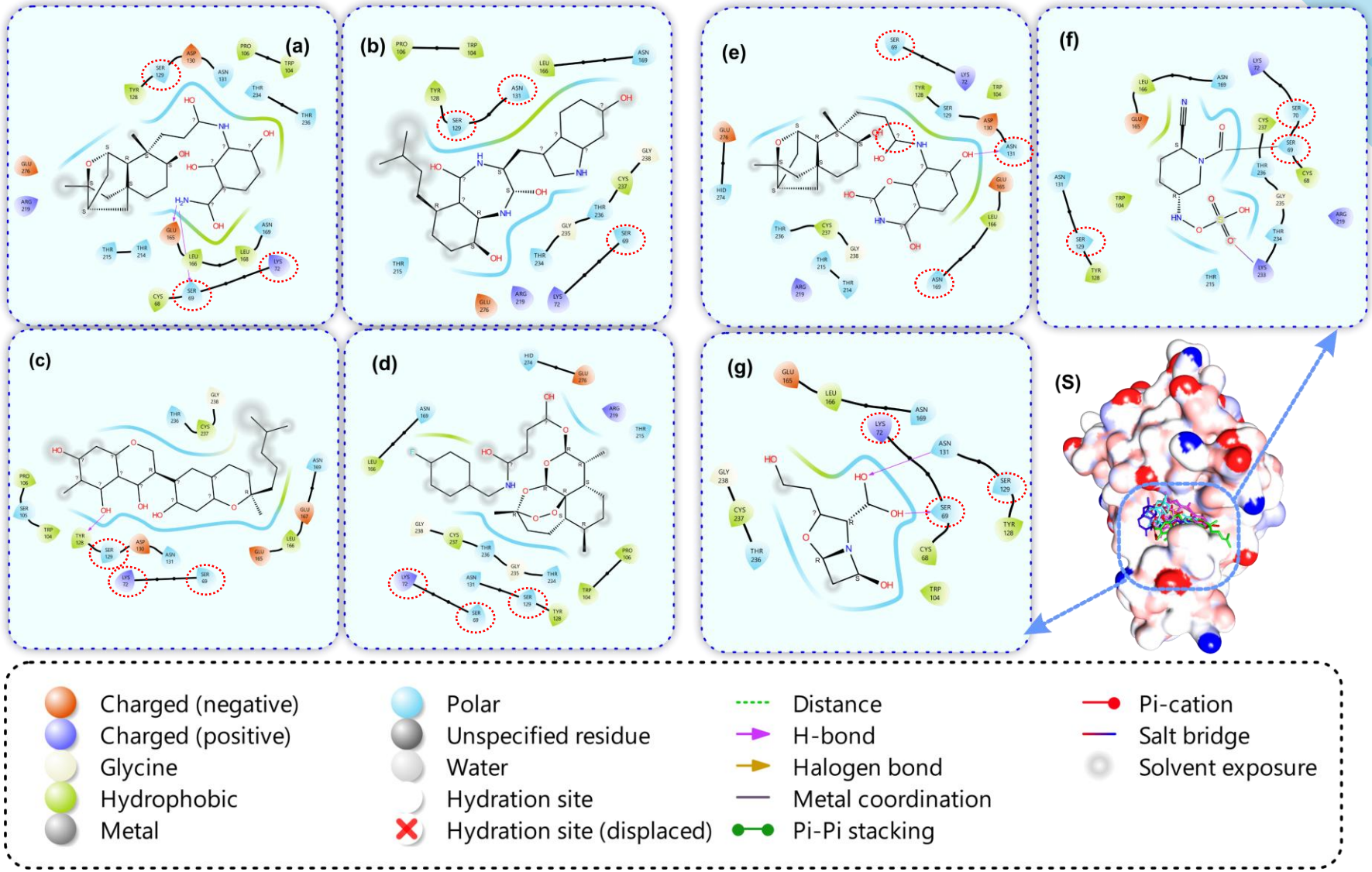


**Figure 7:** Amino acid interactive plots of top-ranked terpenoids and reference inhibitor (ceftaroline) in the active site of KPC-2 β-lactamase. The ligands are displayed as sticks (a) TP64159; (b) TP77265; (c) TP93780; (d) TP124709; (e) TP156670; (f) ceftaroline and (g) Clavulanate

| | TP64159 | TP77265 | TP93780 | TP124709 | TP156670 | Cefotaxime | Clavulanic acid |
|---|---|---|---|---|---|---|---|
| **Molecular weight (g/mol)** | 440.49 | 407.46 | 436.50 | 491.55 | 466.48 | 455.47 | 199.16 |
| **Num. heavy atoms** | 32 | 30 | 32 | 35 | 34 | 30 | 14 |
| **Num. arom. Heavy atoms** | 6 | 9 | 12 | 6 | 10 | 5 | 0 |
| **Num. rotatable bonds** | 6 | 4 | 4 | 8 | 5 | 9 | 2 |
| **Num. H-bond acceptors** | 6 | 4 | 6 | 8 | 7 | 9 | 5 |
| **Hydrogen bond donor** | 4 | 4 | 3 | 1 | 3 | 3 | 2 |
| **Molar Refractivity** | 116.87 | 121.44 | 124.22 | 122.95 | 123.42 | 109.90 | 46.90 |
| **TPSA Å$^2$** | 138.95 | 111.29 | 96.22 | 92.32 | 138.70 | 227.05 | -0.83 |
| **MLogP** | 1.18 | 0.99 | 2.48 | 3.08 | 2.43 | -1.00 | 87.07 |
| **Drug-likeness** | | | | | | | |
| **Lipinski** | Yes | Yes | Yes | Yes | Yes | Yes | Yes |
| **Veber** | Yes | Yes | Yes | Yes | Yes | No | No |
| **Egan** | Yes | Yes | Yes | Yes | No | No | Yes |
| **Ghose** | Yes | Yes | Yes | No | Yes | No | No |
| **Absorption (Probability)** | | | | | | | |
| **HIA** | HIA+ (0.64) | HIA- (0.409) | HIA- (0.56) | HIA+ (0.567) | HIA+ (0.945) | HIA+ (0.074) | HIA+ (0.501) |
| **P-glycoprotein Substrate** | Neg. (0.25) | Neg.(0.48) | Neg. (0.89) | Neg. (0.051) | Neg. (0.737) | Neg. (0.223) | Neg. (0.234) |
| **Distribution (Probability)** | | | | | | | |
| **PPB %** | 74.37 | 90.34 | 90.87 | 88.28 | 88.79 | 37.104 | 21.97 |
| **Metabolism (Probability)** | | | | | | | |
| **CYP450 1A2 Inhibitor** | Neg. (0.04) | Neg. (0.293) | Neg. (0.148) | Neg. (0.131) | Neg. (0.075) | Neg. (0.067) | Neg. (0.015) |
| **CYP450 1A2 Substrate** | Neg. (0.493) | Neg. (0.49) | Neg. (0.36) | Pos. (0.37) | Neg. (0.472) | Neg. (0.373) | Neg. (0.274) |
| **CYP450 3A4 Inhibitor** | Pos. (0.442) | Neg. (0.418) | Neg. (0.52) | Neg. (0.631) | Neg. (0.56) | Neg. (0.181) | Neg. (0.004) |
| **CYP450 3A4 Substrate** | Neg. (0.475) | Neg. (0.589) | Neg. (0.664) | Pos. (0.622) | Neg. (0.494) | Neg. (0.414) | Neg. (0.388) |
| **CYP2C9 inhibitor** | Neg (0.227) | Pos (0.227) | Neg (0.443) | Neg (0.361) | Neg. (0.354) | Neg . (0.193) | Neg. (0.148) |
| **CYP2C9 substrate** | Neg (0.433) | Neg . (0.433) | Neg. (0.371) | Neg . (0.231) | Neg (0.419) | Neg . (0.302) | Neg. (0.268) |
| **Elimination** | | | | | | | |
| **T $_{1/2}$ (Half Life Time)** | 1.372 h | 1.525 h | 2.028 h | 1.413 h | 1.479 h | 0.356 h | 0.495 h |
| **CL (Clearance Rate) mL/min/kg** | 1.295 | 1.861 | 1.767 | 1.43 | 1.477 | 0.792 | 1.364 |
| **Toxicity** | | | | | | | |
| **hERG Blockers** | Neg. (0.298) | Neg. (0.457) | Neg. (0.452) | Neg. (0.527) | Neg. (0.378) | Neg. (0.305) | Pos. (0.086) |
| **SkinSen (Skin sensitization)** | Neg. (0.344) | Neg. (0.249) | Neg. (0.234) | Neg. (0.265) | Neg. (0.267) | Neg. (0.364) | Neg. (0.445) |
| **AMES** | Neg. (0.418) | Neg. (0.418) | Neg. (0.352) | Neg. (0.288) | Neg. (0.328) | Neg. (0.168) | Pos. (0.262) |
| **Carcinogen** | Neg. (0.133) | Neg. (0.9511) | Neg. (0.932) | Neg. (0.870) | Neg. (0.924) | Neg. (0.865) | Neg. (0.55) |
| **Synthetic accessibility** | 5.15 | 4.39 | 4.94 | 6.64 | 5.79 | 4.79 | 3.70 |

**Table 2:** Predicted pharmacokinetics and ADMET properties of the top five terpenoids and reference standard (Imipenem)

(Lipinski et al., 1997; Egan et al., 2000; Ghose et al., 1999; Veber et al., 2002)

**Table 3:** Energy components (kcal/mol) of top five terpenoids bound to *Klebsiella pneumoniae* PBP3 and KPC-2

| SYSTEMS | $\Delta_{VDWAALS}$ | $\Delta_{EEL}$ | $\Delta E_{GB}$ | $\Delta E_{SUR}$ | $\Delta G_{GAS}$ | $\Delta G_{SOLV}$ | $\Delta_{TOTAL}$ |
|---|---|---|---|---|---|---|---|
| | ***Klebsiella pneumoniae* PBP3** | | | | | | |
| **8GPW_TP64159** | –18.29 ± 1.50 | –7.8 ± 5.92 | 18.64 ± 2.74 | –2.55 ± 0.68 | –26.17 ± 6.21 | 16.08 ± 2.83 | –10.09 ± 6.83 |
| **8GPW_TP77265** | –35.05 ± 0.46 | –11.00 ± 0.49 | 28.45 ± 0.15 | –4.86 ± 0.26 | –46.04 ± 1.11 | 23.59 ± 0.30 | –22.45 ±1.14 |
| **8GPW_TP93780** | –33.01 ± 0.71 | –11.59 ± 4.62 | 24.62 ± 2.18 | –4.43 ± 0.05 | –44.59 ± 4.72 | 20.19 ± 2.19 | **–24.40 ± 5.20** |
| **8GPW_TP124709** | –32.16 ± 1.41 | –9.90 ± 3.96 | 26.27 ± 1.68 | –4.54 ± 0.10 | –42.06 ± 4.34 | 21.73 ± 1.68 | –20.33 ± 4.65 |
| **8GPW_TP156670** | –30.69 ± 5.77 | –10.88 ± 3.20 | 22.15 ± 0.25 | –4.04 ± 0.28 | –41.57 ± 3.48 | 19.11 ± 0.37 | **–23.46 ± 3.50** |
| **8GPW_Ceftaroline** | –29.38 ± 1.51 | –523.59 ± 41.49 | 546.15 ± 36.45 | –5.01 ± 0.59 | –552.96 ± 4.67 | 541.15 ± 36.23 | –21.82 ± 8.64 |
| | ***Klebsiella pneumoniae* KPC-2 β-Lactamase** | | | | | | |
| **6B1F_TP64159** | –22.12 ± 1.47 | –6.06 ± 6.08 | 17.58 ± 3.06 | –2.98 ± 0.03 | –26.38 ± 6.36 | 14.60 ± 3.06 | –13.58 ± 7.06 |
| **6B1F_TP77265** | –11.26 ± 1.51 | –6.24 ± 1.43 | 11.86 ± 1.25 | –1.51 ± 0.55 | –17.50 ± 2.24 | 10.35 ± 1.36 | –7.15 ± 2.62 |
| **6B1F_TP93780** | –23.12 ± 1.58 | –5.94 ± 4.21 | 16.81 ± 1.93 | –3.13 ± 0.03 | –29.06 ± 4.55 | 13.68 ± 1.93 | **–15.38 ± 4.09** |
| **6B1F_TP124709** | –19.70 ± 0.84 | –3.92 ± 3.59 | 12.86 ± 1.43 | –2.79 ± 0.17 | –23.62 ± 3.84 | 10.06 ± 1.44 | –13.56 ± 4.10 |
| **6B1F_TP156670** | –22.33 ± 0.61 | –24.12 ± 3.21 | 32.77 ± 1.43 | –3.14 ± 0.16 | –46.46 ± 3.47 | 29.63 ± 1.44 | **–16.83 ± 3.75** |
| **6B1F_Clavulanic acid** | –9.12 ± 4.14 | –46.67 ± 24.18 | 46.58 ± 24.01 | –1.65 ± 1.08 | –55.79 ± 24.62 | 44.94 ± 24.04 | –10.85 ± 34.40 |

*$\Delta_{VDWAALS}$: Change in van der Waals energy; $\Delta_{EEL}$: Change in electrostatic energy; $\Delta_{EGB}$: Change in electrostatic potential energy; $\Delta_{ESUR}$: Change in surface energy; $\Delta_{GGAS}$: Change in the Gibbs free energy of the gas phase; $\Delta G_{SOLV}$: Change in Gibbs free energy of solvation; $\Delta_{TOTAL}$: Total energy change*

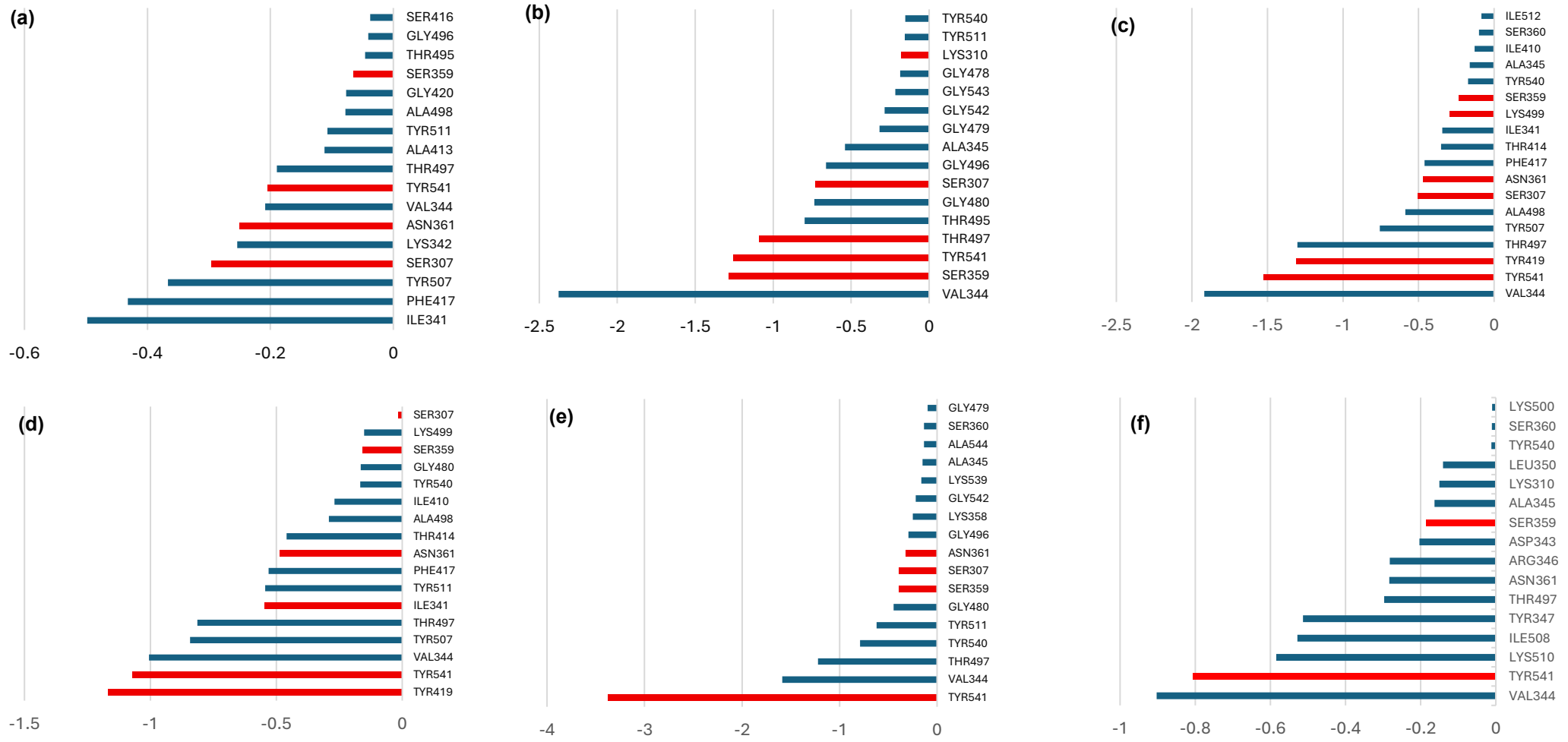


**Figure 8:** Per-residue contribution plots to the total binding free energy of top five terpenoids: (a) TP64159; (b) TP77265; (c) TP93780; (d) TP124709; (e) TP156670; (f) ceftaroline for the active site of *K. pneumoniae* PBP3 (Red coloured bars represent active site residues).

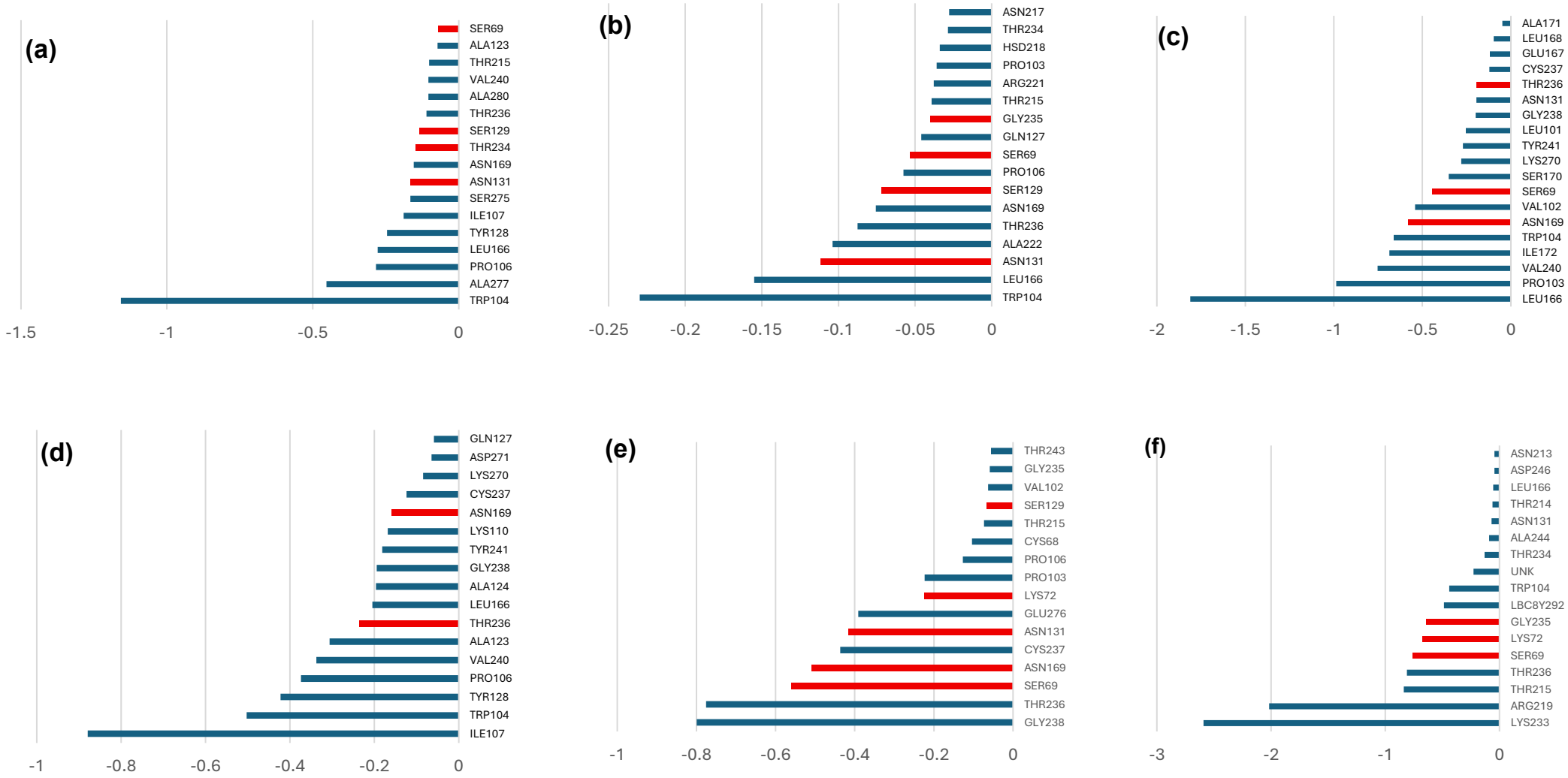


**Figure 9:** Per-residue contribution plots to the total binding free energy of top five terpenoids: (a) TP64159; (b) TP77265; (c) TP93780; (d) TP124709; (e) TP156670; (f) clavulanic acid for the active site of KPC-2 beta-lactamase (Red coloured bars represent active site residues).

**Table 4:** Post-MD structural analysis data of the unbound, top five terpenoids and reference standard bound to the active site *Klebsiella pneumoniae* PBP3 and KPC-2 beta-lactamase

| Systems | RMSD | RMSF | RoG | SASA | Hbond |
|---|---|---|---|---|---|
| | *Klebsiella pneumoniae* PBP3 | | | | |
| **8gpw_apo** | 1.45 ± 1.64 | 0.77 ± 5.34 | 21.57 ± 0.63 | 17976.97 ± 235.89 | 93.13 ± 7.80 |
| **8gpw_TP64159** | 1.38 ± 1.58 | 0.78 ± 5.74 | 21.52 ± 0.69 | 18011.40 ± 216.80 | 93.36 ± 7.74 |
| **8gpw_ TP77265** | 1.74 ± 2.89 | 0.93 ± 6.30 | 21.63 ± 1.21 | 18501.91 ± 345.92 | 95.11 ± 8.06 |
| **8gpw_TP93780** | 1.52 ± 1.96 | 0.77 ± 6.50 | 21.51 ± 0.67 | 17997.95 ± 219.41 | 93.77 ± 7.79 |
| **8gpw_TP124709** | 1.44 ± 1.75 | 0.71 ± 5.80 | 21.50 ± 0.61 | 17829.05 ± 222.07 | 96.50 ± 7.98 |
| **8gpw_TP156670** | 1.42 ± 1.47 | 0.73 ± 5.28 | 21.55 ± 0.67 | 18205.94 ± 251.10 | 92.73 ± 7.80 |
| **8gpw_18C** | 1.33 ± 1.36 | 0.74 ± 5.69 | 21.48 ± 0.56 | 17871.35 ± 207.34 | 95.11 ± 7.94 |
| **8gpw_Ceftaroline** | **1.55 ± 1.97** | **0.84 ± 6.21** | **21.51 ± 0.67** | **18242.82 ± 272.19** | **93.69 ± 7.61** |
| | *Klebsiella pneumoniae* KPC-2 beta-lactamase | | | | |
| **6B1F_apo** | 1.91 ± 5.08 | 1.00 ± 12.83 | 18.25 ± 1.20 | 12315.55 ± 219.40 | 64.54 ± 6.54 |
| **6B1F_TP64159** | 1.69 ± 3.27 | 0.87 ± 5.15 | 18.26 ± 1.47 | 12373.04 ± 234.14 | 64.13 ± 6.55 |
| **6B1F_TP77265** | 1.70 ± 3.37 | 0.95 ± .9.04 | 18.22 ± 1.13 | 12560.25 ± 409.73 | 64.28 ± 6.46 |
| **6B1F_TP93780** | 1.56 ± 4.67 | 0.99 ± 12.58 | 18.24 ± 1.57 | 12466.74 ± 264.95 | 64.56 ± 6.63 |
| **6B1F_TP124709** | 1.79 ± 6.60 | 1.00 ± 11.06 | 18.30 ± 1.51 | 12843.44 ± 430.16 | 62.32 ± 6.59 |
| **6B1F_TP156670** | 1.59 ± 2.55 | 0.80 ± 7.65 | 18.24 ± 1.00 | 12387.44 ± 159.26 | 63.89 ± 6.53 |
| **6B1F_WCK 4234** | 1.75 ± 3.14 | 0.95 ± 9.04 | 18.22 ± 1.13 | 12560.25 ± 409.73 | 64.28 ± 6.46 |
| **6B1F_Clavulanate** | 1.75 ± 4.01 | 0.95 ± 10.93 | 18.23 ± 1.53 | 12458.49 ± 222.66 | 65.79 ± 6.97 |

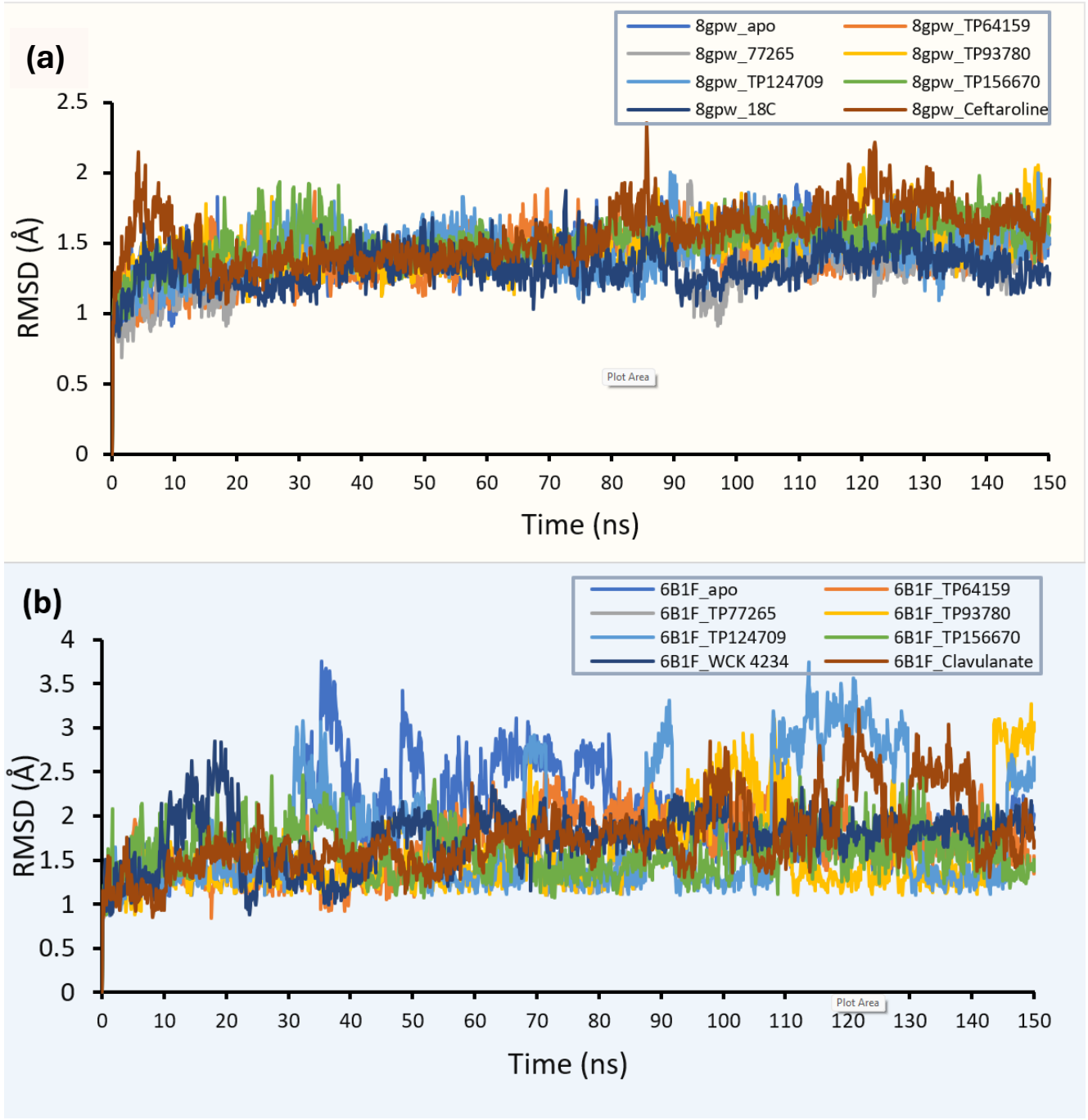


| | Systems | RMSD (Å) |
|---|---|---|
| | 8gpw_apo | 1.45 ± 1.64 |
| **T1** | 8gpw_TP64159 | 1.38 ± 1.58 |
| **T2** | 8gpw_ TP77265 | 1.74 ± 2.89 |
| **T3** | **8gpw_TP93780** | **1.52 ± 1.96** |
| **T4** | 8gpw_TP124709 | 1.44 ± 1.75 |
| **T5** | **8gpw_TP156670** | **1.42 ± 1.47** |
| | 8gpw_18C | 1.33 ± 1.36 |
| | 8gpw_Ceftaroline | 1.55 ± 1.97 |

| | Systems | RMSD (Å) |
|---|---|---|
| | 6B1F_apo | 1.91 ± 5.08 |
| **T1** | 6B1F_TP64159 | 1.69 ± 3.27 |
| **T2** | 6B1F_TP77265 | 1.70 ± 3.37 |
| **T3** | **6B1F_TP93780** | **1.56 ± 4.67** |
| **T4** | 6B1F_TP124709 | 1.79 ± 6.60 |
| **T5** | 6B1F_TP156670 | 1.59 ± 2.55 |
| | 6B1F_WCK 4234 | 1.75 ± 3.14 |
| | 6B1F_Clavulanate | 1.75 ± 4.01 |

**Figure 10:** Root-mean-square deviation (RMSD) of the of MD simulation trajectories of the top five terpenoids and reference standards docked to the binding site of **(a)** *K. pneumoniae* PBP3 **(b)** KPC-2 beta-lactamase

(Maruyama et al., 2023)

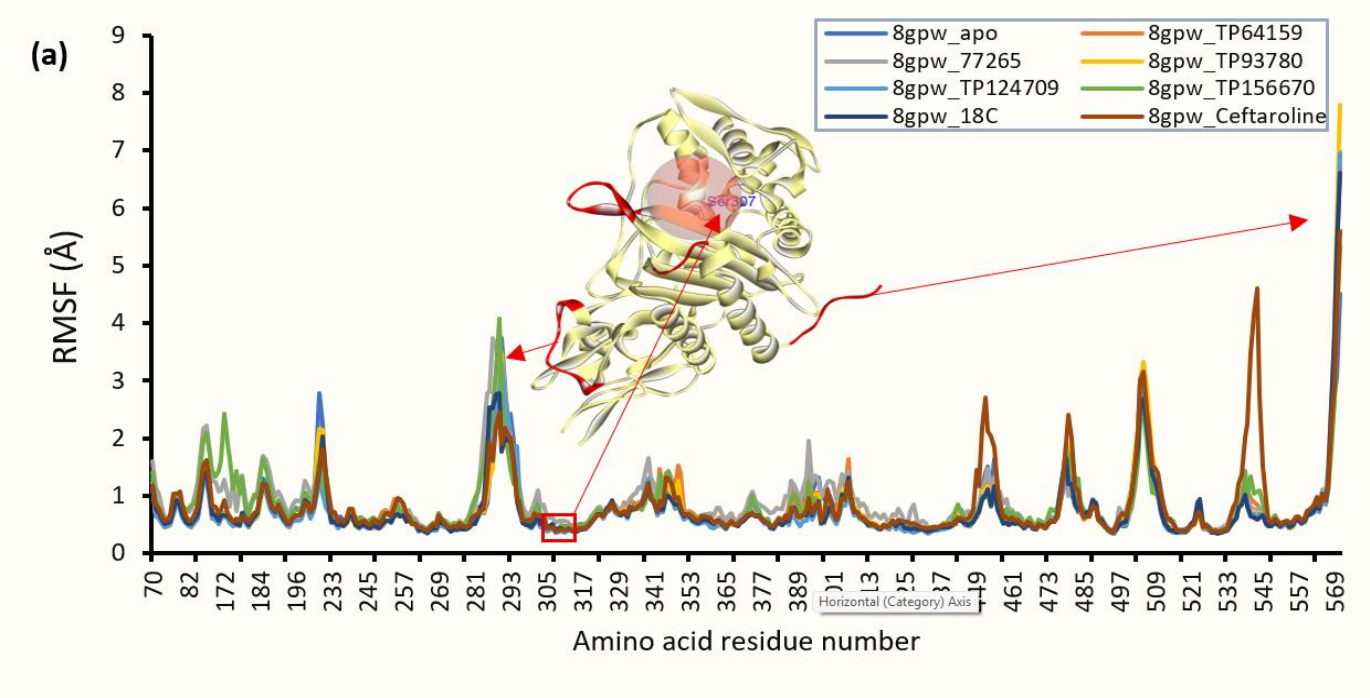


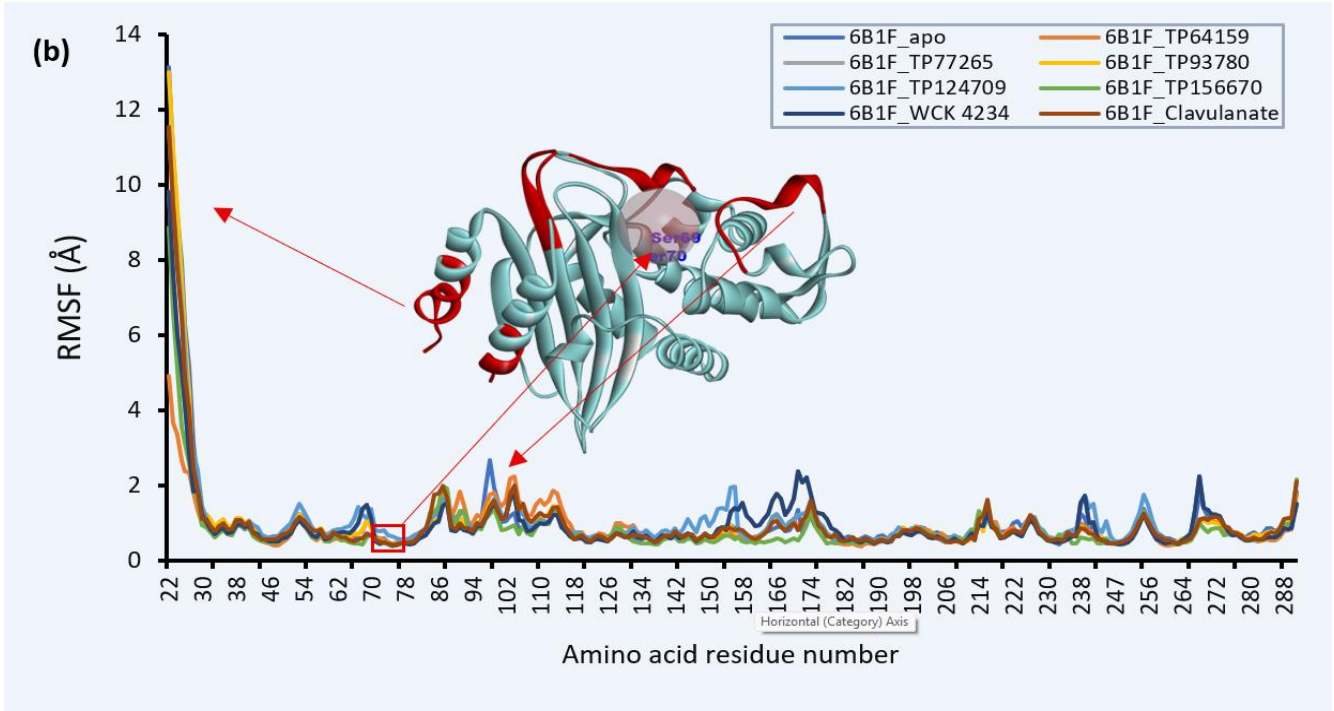


| | Systems | RMSF (Å) |
|---|---|---|
| | 8gpw_apo | **0.77 ± 5.34** |
| **T1** | 8gpw_TP64159 | 0.78 ± 5.74 |
| **T2** | 8gpw_ TP77265 | 0.93 ± 6.30 |
| **T3** | 8gpw_TP93780 | **0.77 ± 6.50** |
| **T4** | 8gpw_TP124709 | 0.71 ± 5.80 |
| **T5** | 8gpw_TP156670 | **0.73 ± 5.28** |
| | 8gpw_18C | 0.74 ± 5.69 |
| | 8gpw_Ceftaroline | **0.84 ± 6.21** |

| | Systems | RMSF (Å) |
|---|---|---|
| | 6B1F_apo | 1.00 ± 12.83 |
| **T1** | 6B1F_TP64159 | 0.87 ± 5.15 |
| **T2** | 6B1F_TP77265 | 0.95 ± .9.04 |
| **T3** | 6B1F_TP93780 | 0.99 ± 12.58 |
| **T4** | 6B1F_TP124709 | 1.00 ± 11.06 |
| **T5** | 6B1F_TP156670 | 0.80 ± 7.65 |
| | 6B1F_WCK 4234 | 0.95 ± 9.04 |
| | 6B1F_Clavulanate | **0.95 ± 10.93** |

(Pitera, 2014)

**Figure 11:** Per residue root mean square fluctuations (RMSF) plots of the of MD simulation trajectories of the top five terpenoids and reference standards docked to the binding site of **(a)** *K. pneumoniae* PBP3 **(b)** KPC-2 beta-lactamase

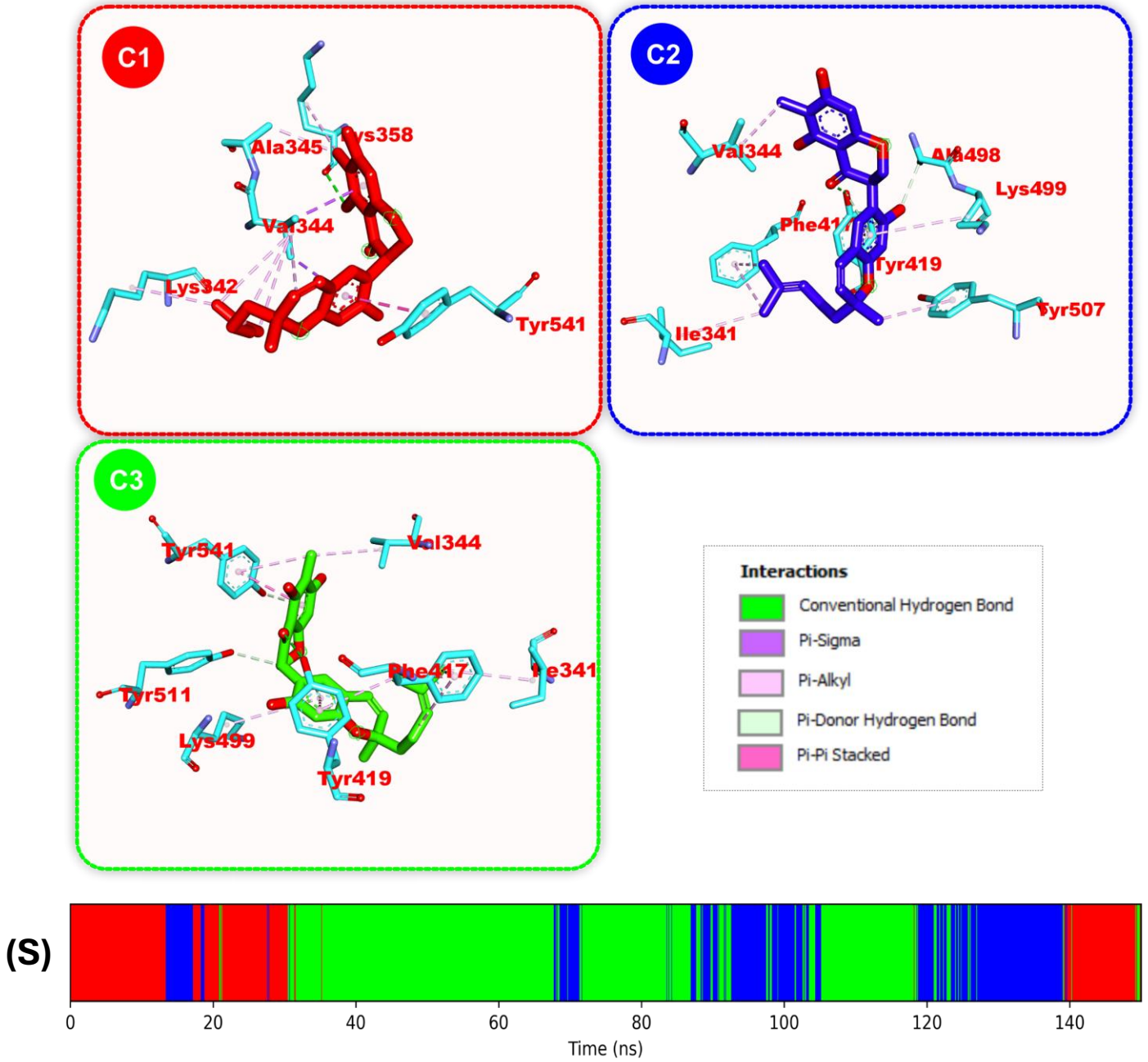


(Shao et al., 2007).

**Figure 13:** Interactive plots of representative conformation from the clusters **(C1-C3)** obtained from the clustering analysis of MD simulation trajectories **PBP3_TP93780** system; **(s)** linear projection of clusters made for the trajectory, every barline represents a frame and the colour, a cluster number (C1: red; C2: blue, C3: green)

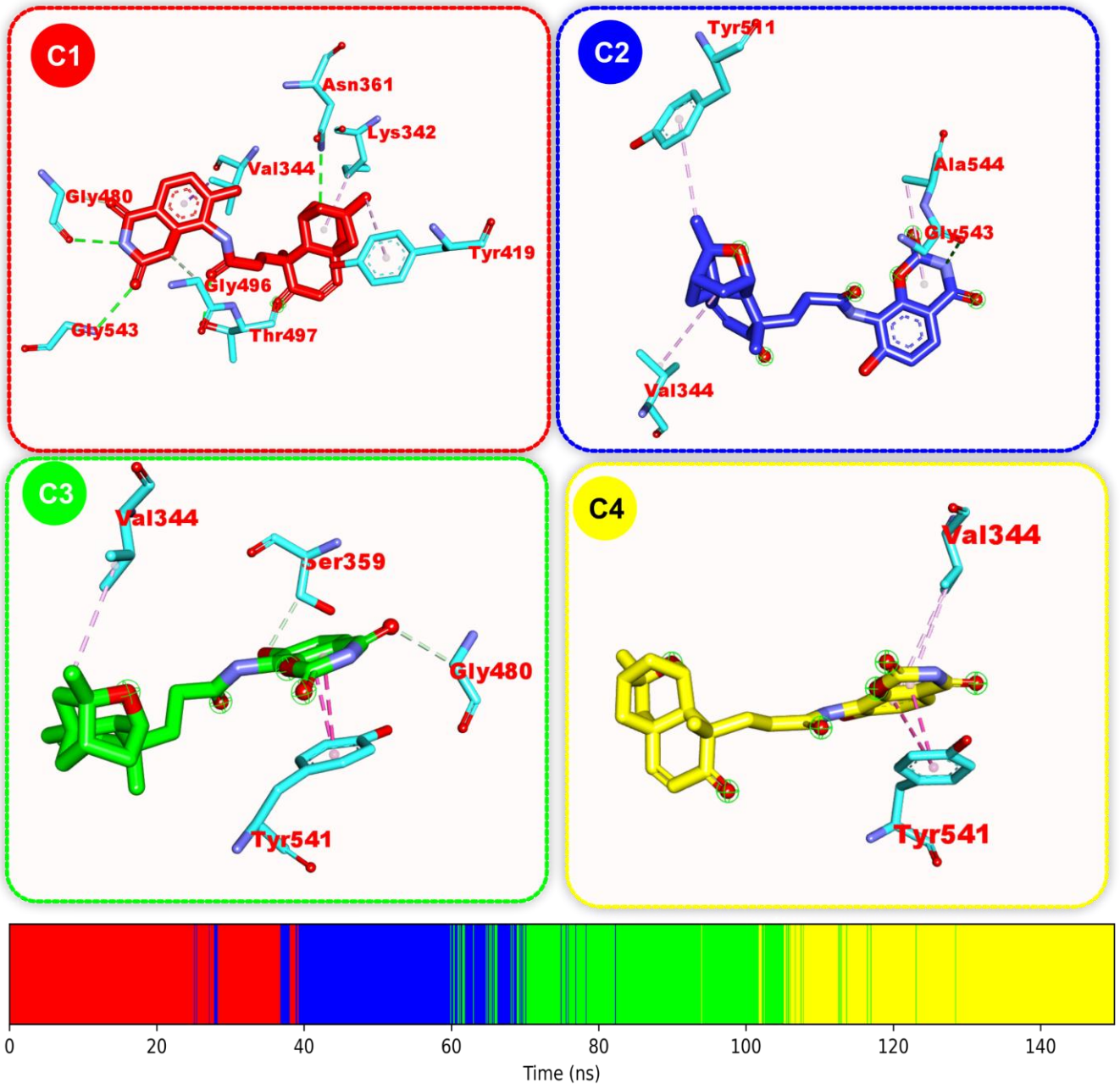


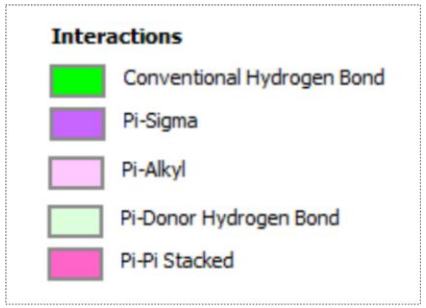


**Figure 14:** 3D Interactive plots of representative conformation from the clusters **(C1-C4)** obtained from the clustering analysis of MD simulation trajectories **PBP3_TP156670** system **(s);** linear projection of clusters made for the trajectory, every barline represents a frame and the colour a cluster number (C1: red; C2: blue, C3: green and C4: yellow).

(Shao et al., 2007).

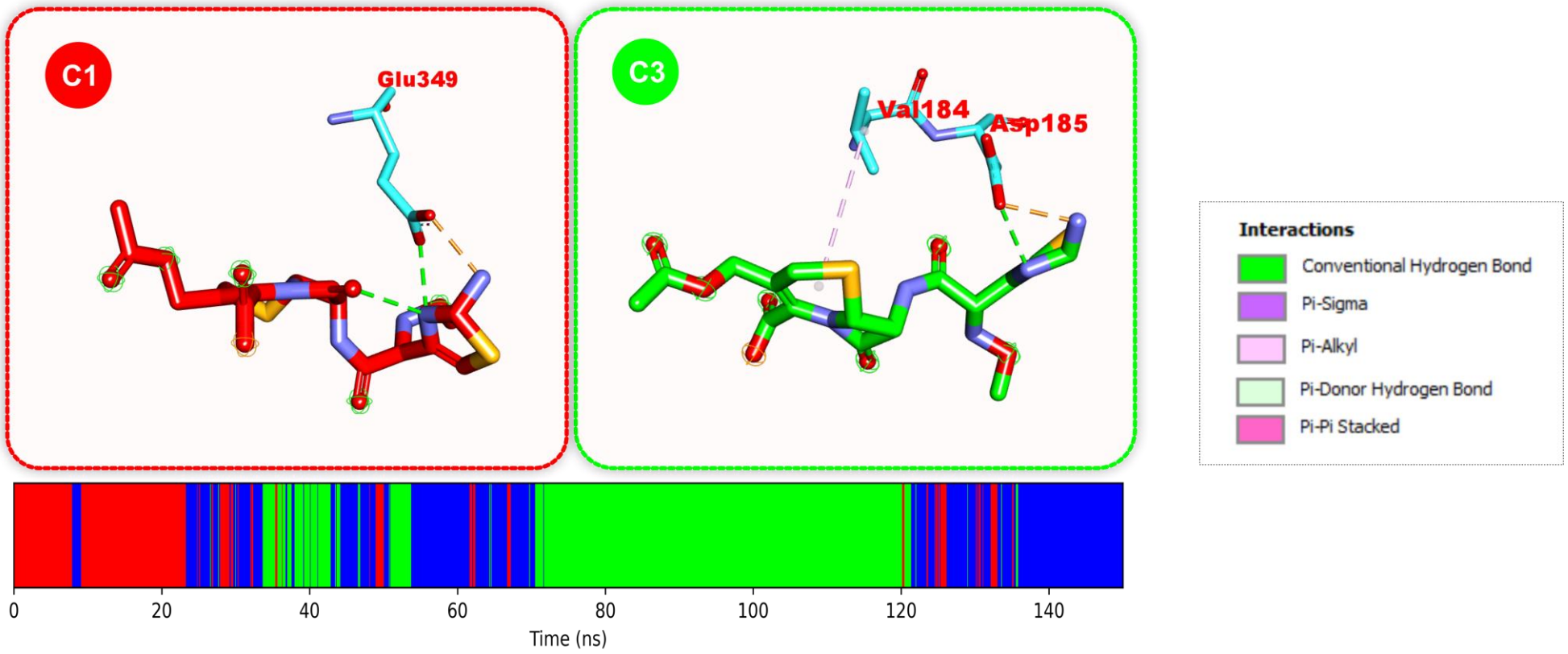


**Figure 15:** Interactive plots of representative conformation from the clusters **(C1-C3)** obtained from the clustering analysis of MD simulation trajectories **PBP3_Ceftaroline** system **(s);** linear projection of clusters made for the trajectory, every barline represents a frame and the colour a cluster number (C1: red; C2: blue, C3: green)

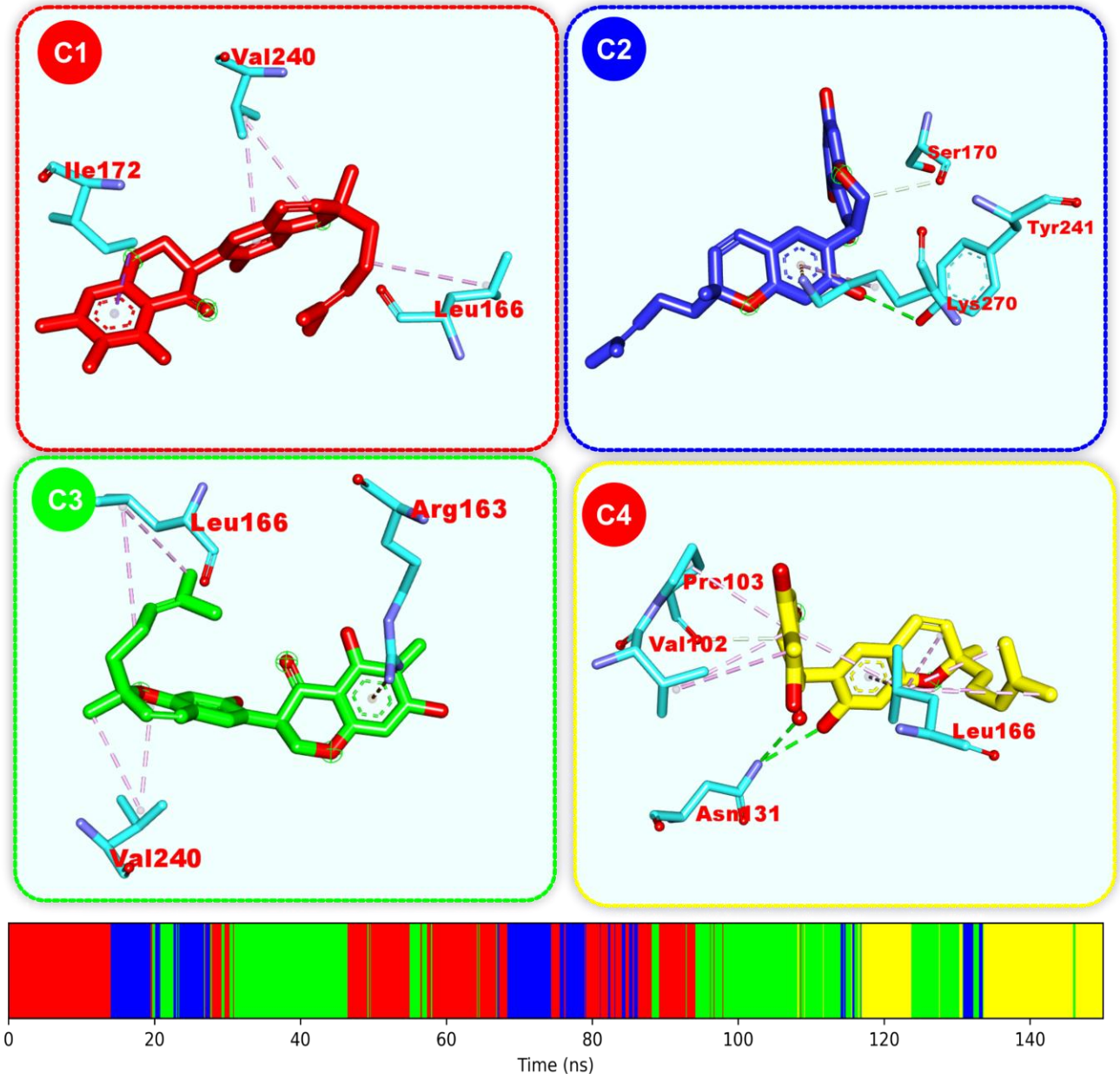


**Figure 16:** Interactive plots of representative conformation from the clusters **(C1-C4)** obtained from the clustering analysis of MD simulation trajectories **KPC-2_TP93780** system **(s);** linear projection of clusters made for the trajectory, every barline represents a frame and the colour a cluster number (C1: red; C2: blue, C3: green, C4: yellow) **(D)** Per-residue contribution to the total binding free energy of PBP5_Imipenem (Red coloured bars represent active site residues

(Shao et al., 2007).

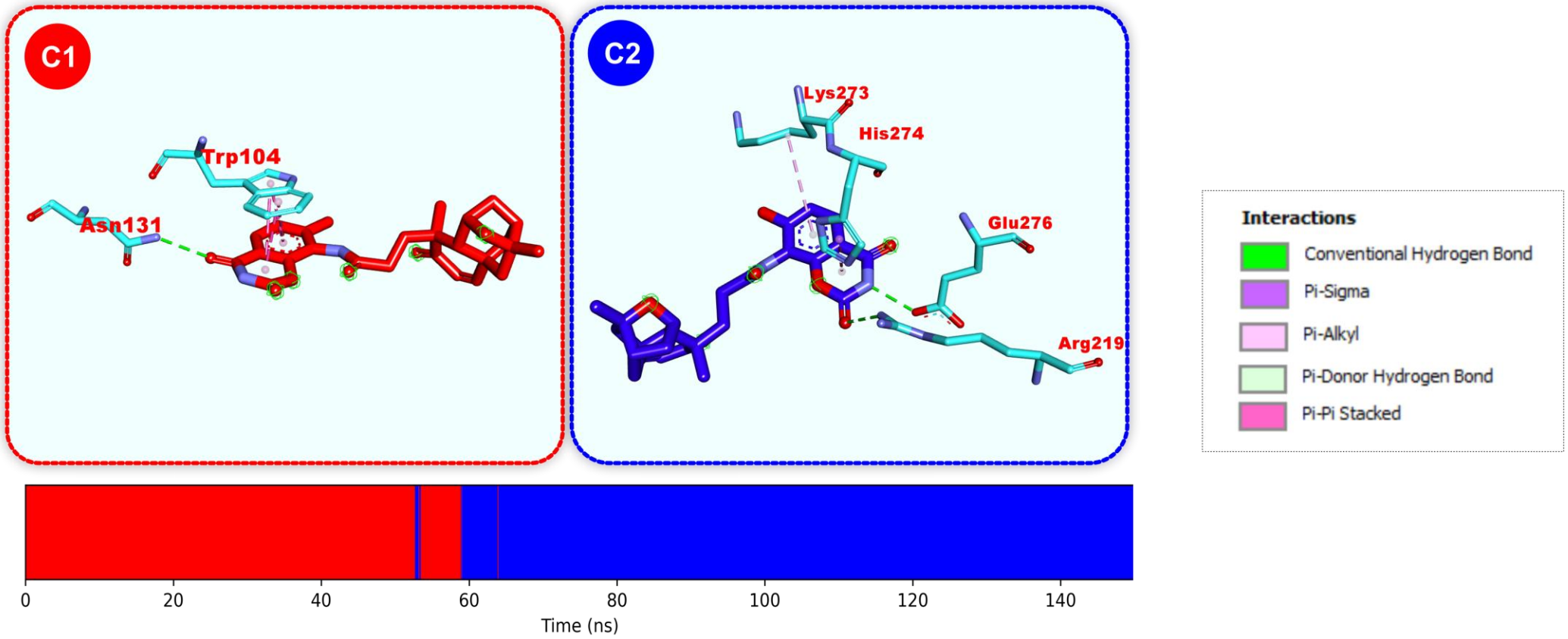


**Figure 17:** Interactive plots of representative conformation from the clusters **(C1-C2)** obtained from the clustering analysis of MD simulation trajectories **KPC-2_P156670** system **(s);** linear projection of clusters made for the trajectory, every barline represents a frame and the colour a cluster number (C1: red; C2: blue)

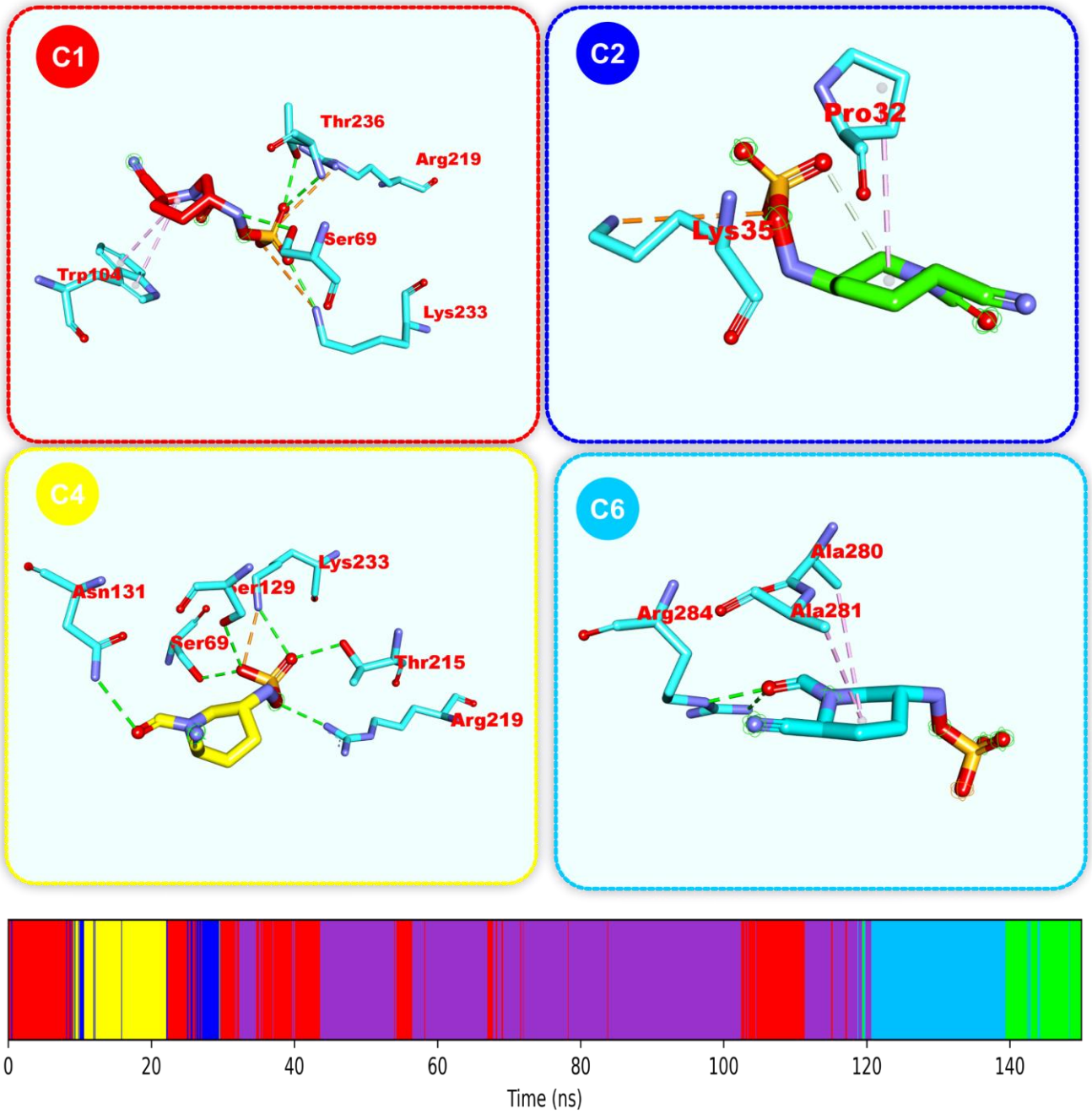


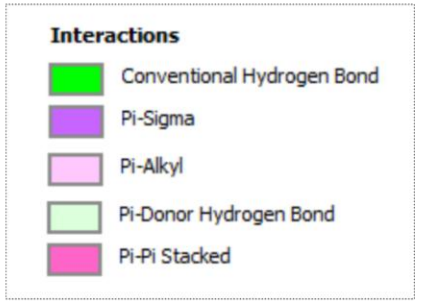


**Figure 18:** Interactive plots of representative conformation from the clusters **(C1-C6)** obtained from the clustering analysis of MD simulation trajectories **KPC-2_Clavulanate** system **(s);** linear projection of clusters made for the trajectory, every barline represents a frame and the colour a cluster number (C1: red; C2: blue, C3: green, C4: yellow, C5: C6: light blue) **(D)** Per-residue contribution to the total binding free energy of PBP5_Imipenem (Red coloured bars represent active site residues

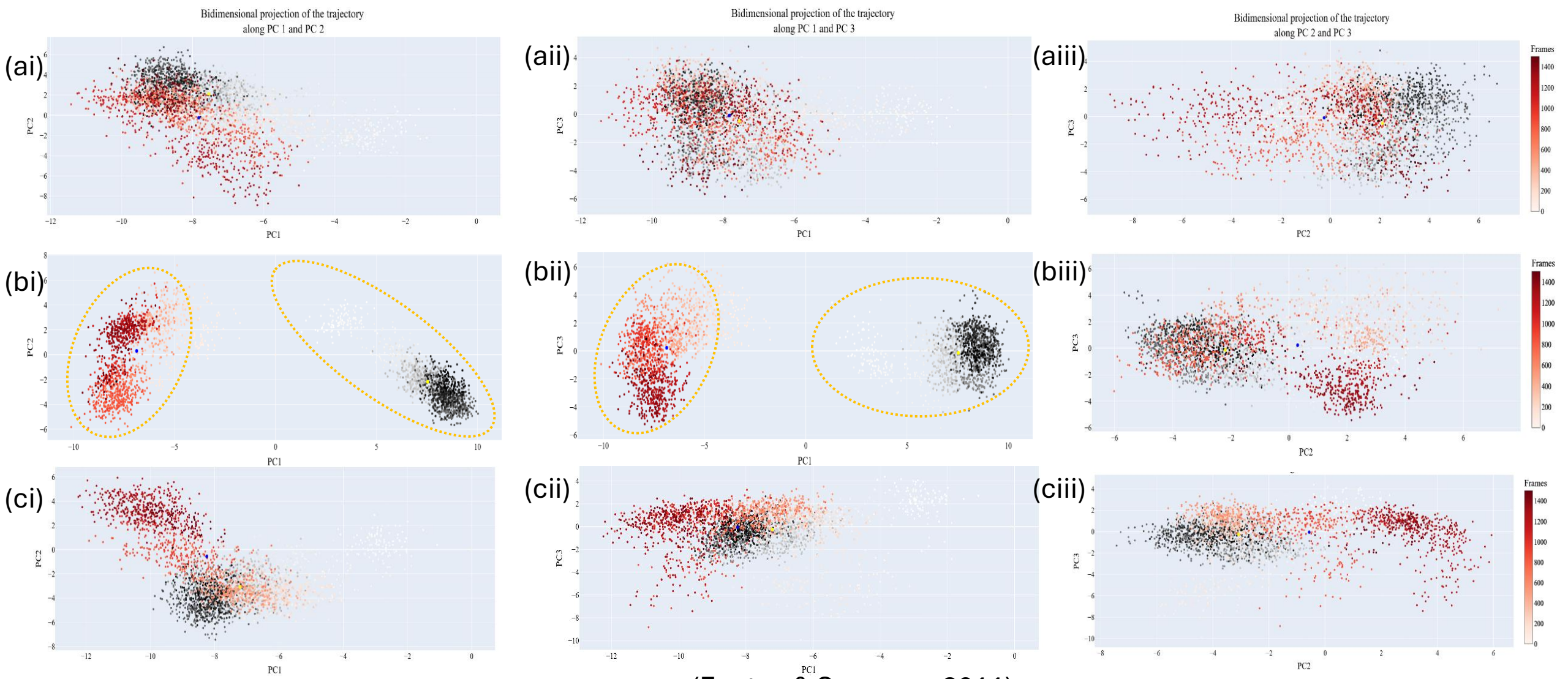


(Fontes & Soneson, 2011)

**Figure 19:** The eigenvectors projections of the unbound and ligands: (a) TP93780 (b) TP156670 and (c) ceftaroline bound to the active of *K. pneumoniae* PBP3 (a) bound *K. pneumoniae* PBP3. In the plots, small dots transitioning from white to black represent frames from the unbound structure, while dots changing from light red to deep red represent frames from the **ligand bound** structures

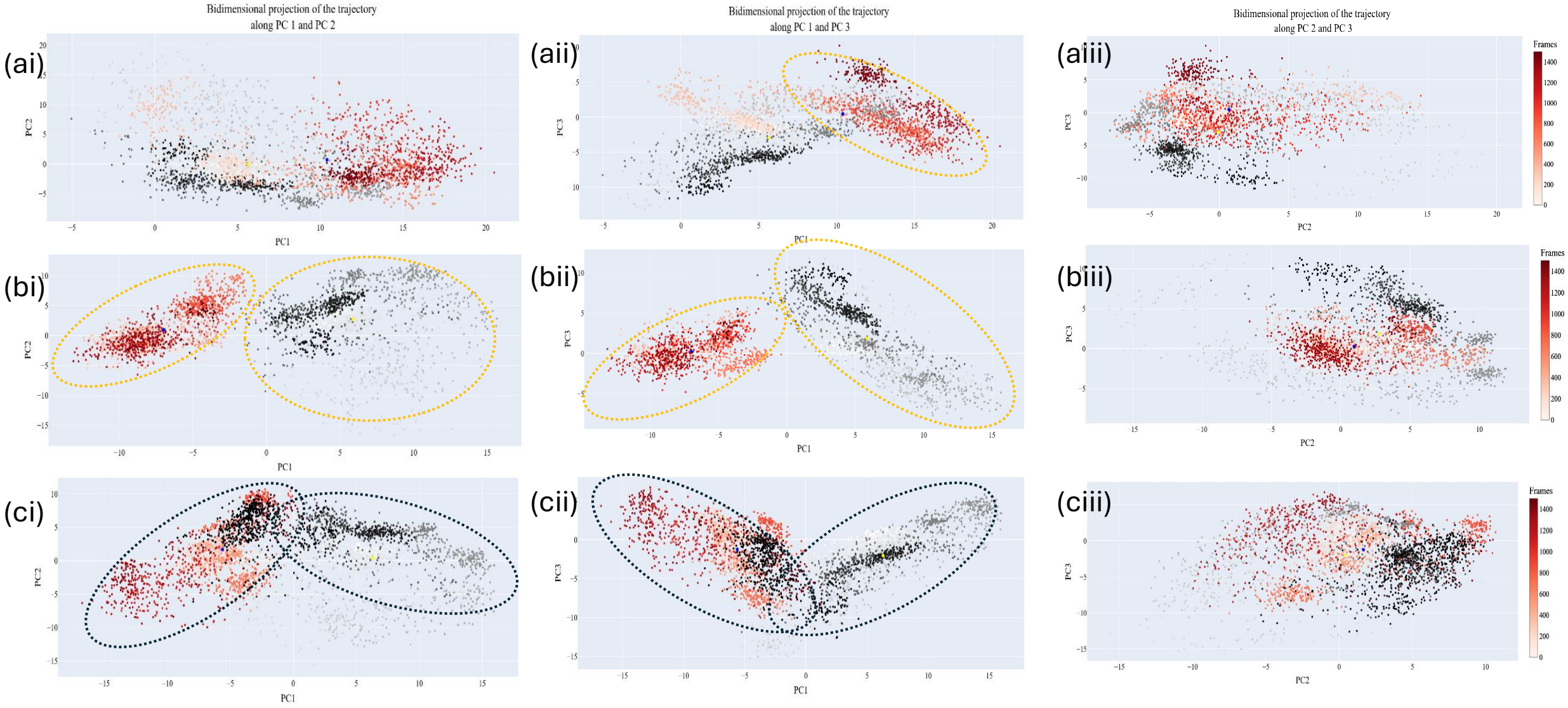


**Figure 20:** The eigenvectors projections of the unbound and ligands: (a) TP93780 (b) TP156670 and (c) Clavulanate bound to the active of KPC-2 beta-lactamase. In the plots, small dots transitioning from white to black represent frames from the **unbound** structure, while dots changing from light red to deep red represent frames from the **ligand bound** structures**.**

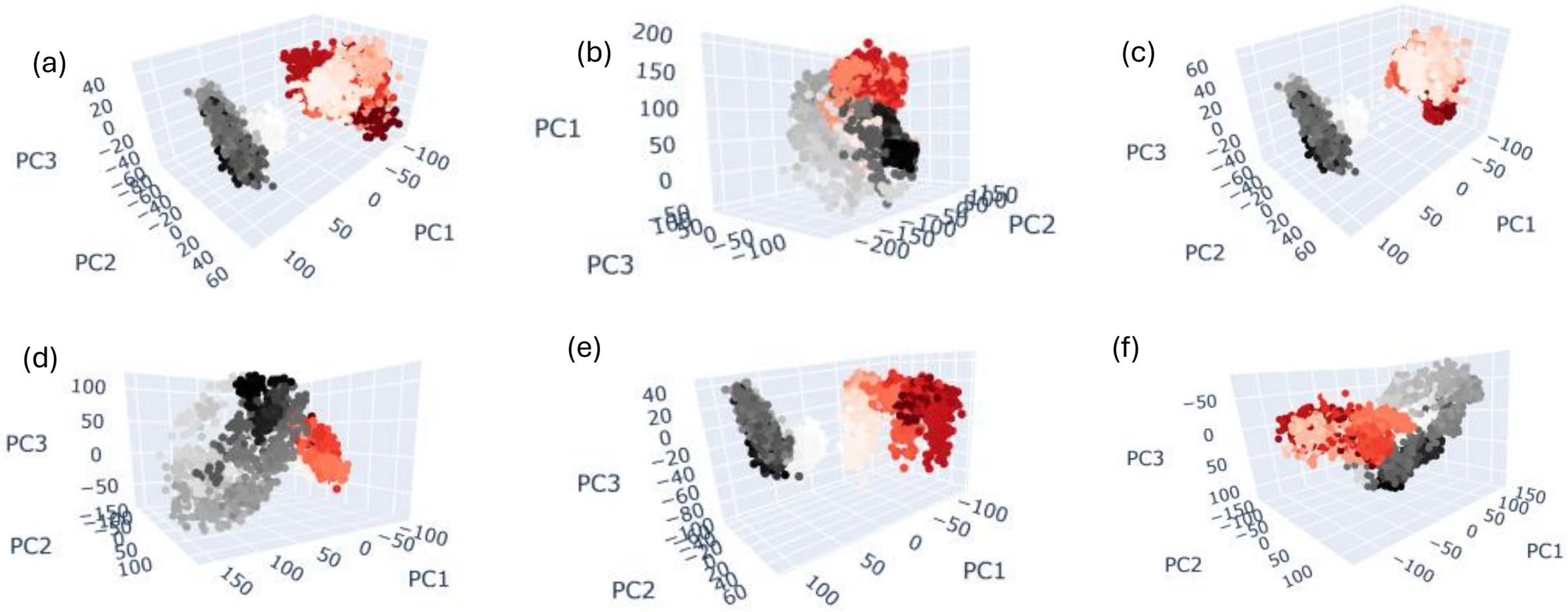


Figure 21: The 3D projection of the first three eigenvectors (PC1-PC2-PC3) of the unbound and ligand bound structures (a) 8gpw_TP93780 (b) 6B1F_TP93780 (c) 8gpw_TP156670 (d) 6B1F_TP156670 (e) 8gpw_Ceftaroline (f) 6B1F_Clavulanate. Red line shows the cumulative variance retained by the eigenvectors.

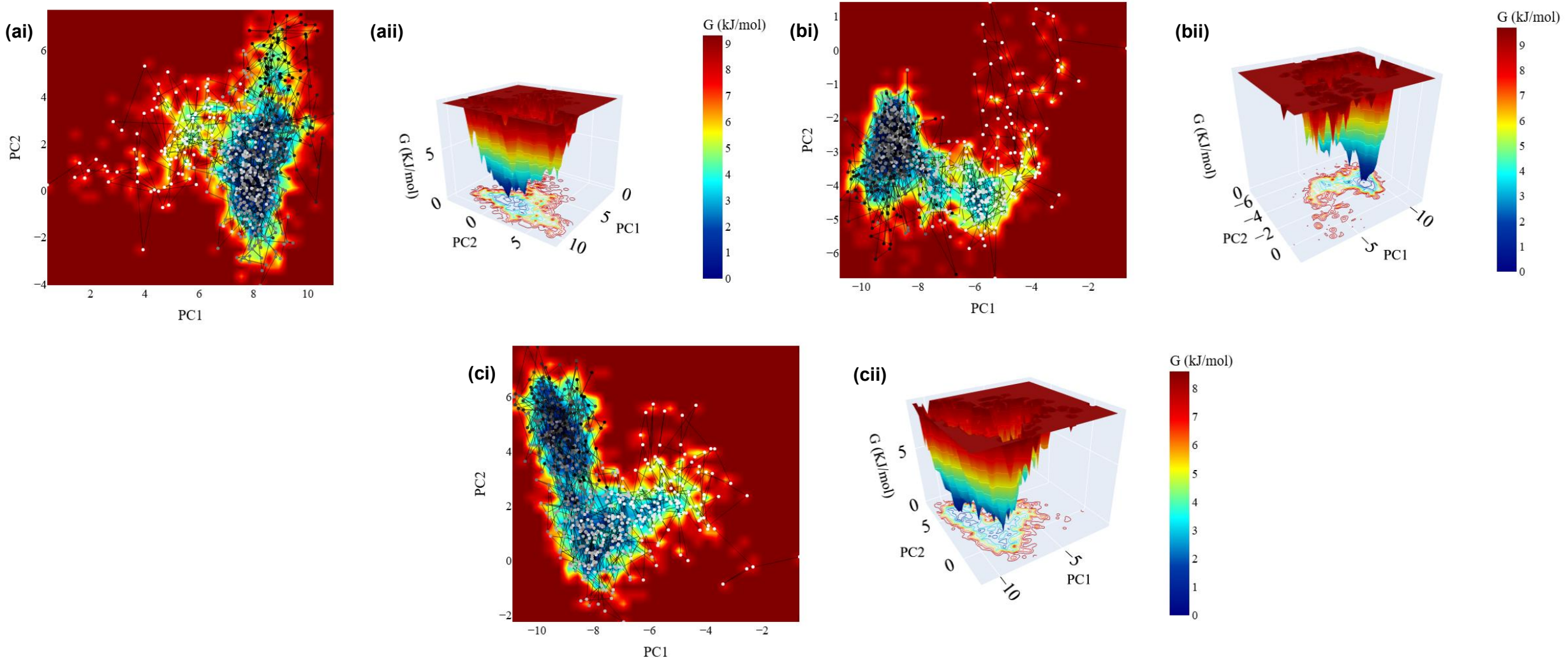


Figure 22: The (i) 2D and (ii) 3D conformational free-energy landscapes of the system projected onto the first two eigenvectors (PC1-PC2) of the ligand bound structures (a) 8gpw_TP93780 (b) 8gpw_TP156670 (c) 8gpw_Ceftaroline. In 2D plots, the dots with colours ranging from white to black, represent frames. The energy levels (G, in kJ/mol) are represented on a colour mapping following a red-yellow-blue scale, with deep blue corresponding to the global minimum (0.0 kJ/mol) as obtained from the gmx sham command.

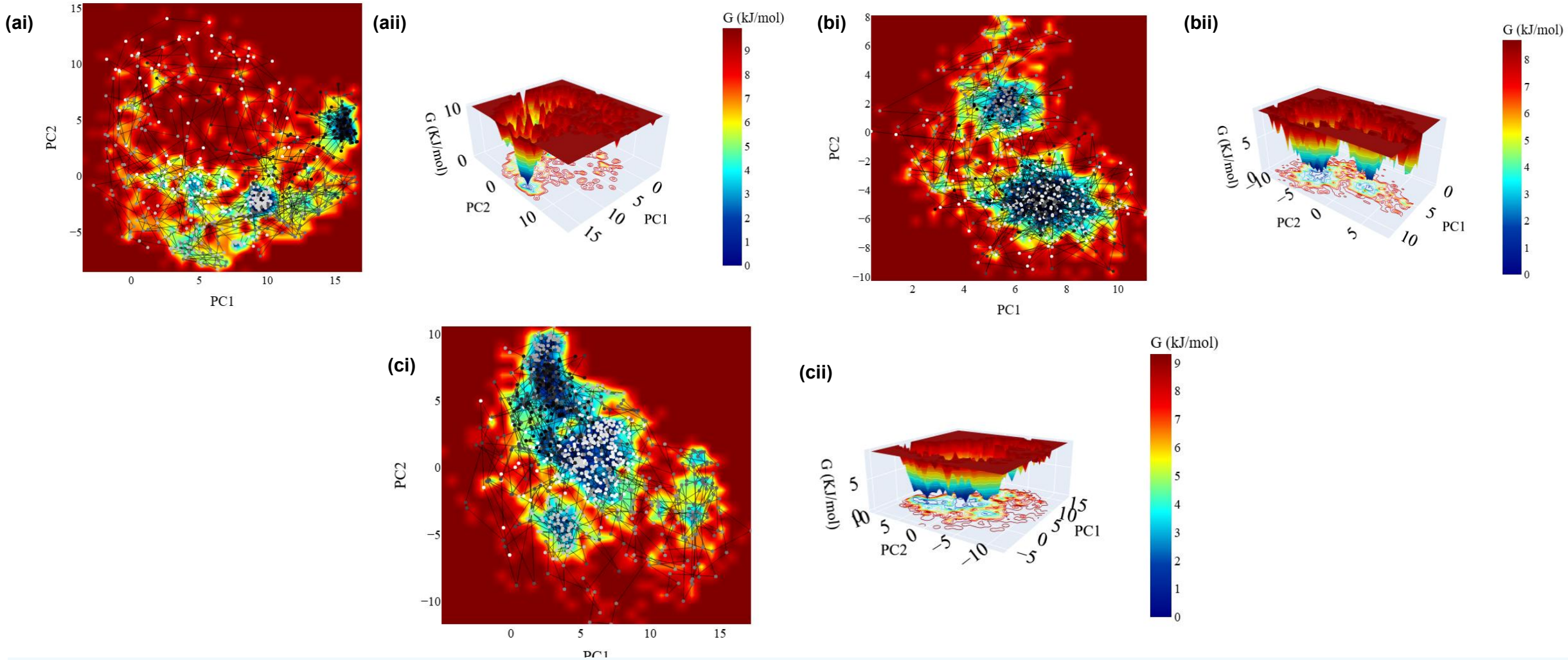


Figure 23: The (i) 2D and (ii) 3D conformational free-energy landscapes of the system projected onto the first two eigenvectors (PC1-PC2) of the ligand bound structures (a) 6B1F_TP93780 (b) 6B1F_TP156670 (c) 6B1F_Clavulanate. The dots with colours ranging from white to black, represent frames. In 2D plots, the dots with colours ranging from white to black, represent frames. The energy levels (G, in kJ/mol) are represented on a colour mapping following a red-yellow-blue scale, with deep blue corresponding to the global minimum (0.0 kJ/mol) as obtained from the gmx sham command.

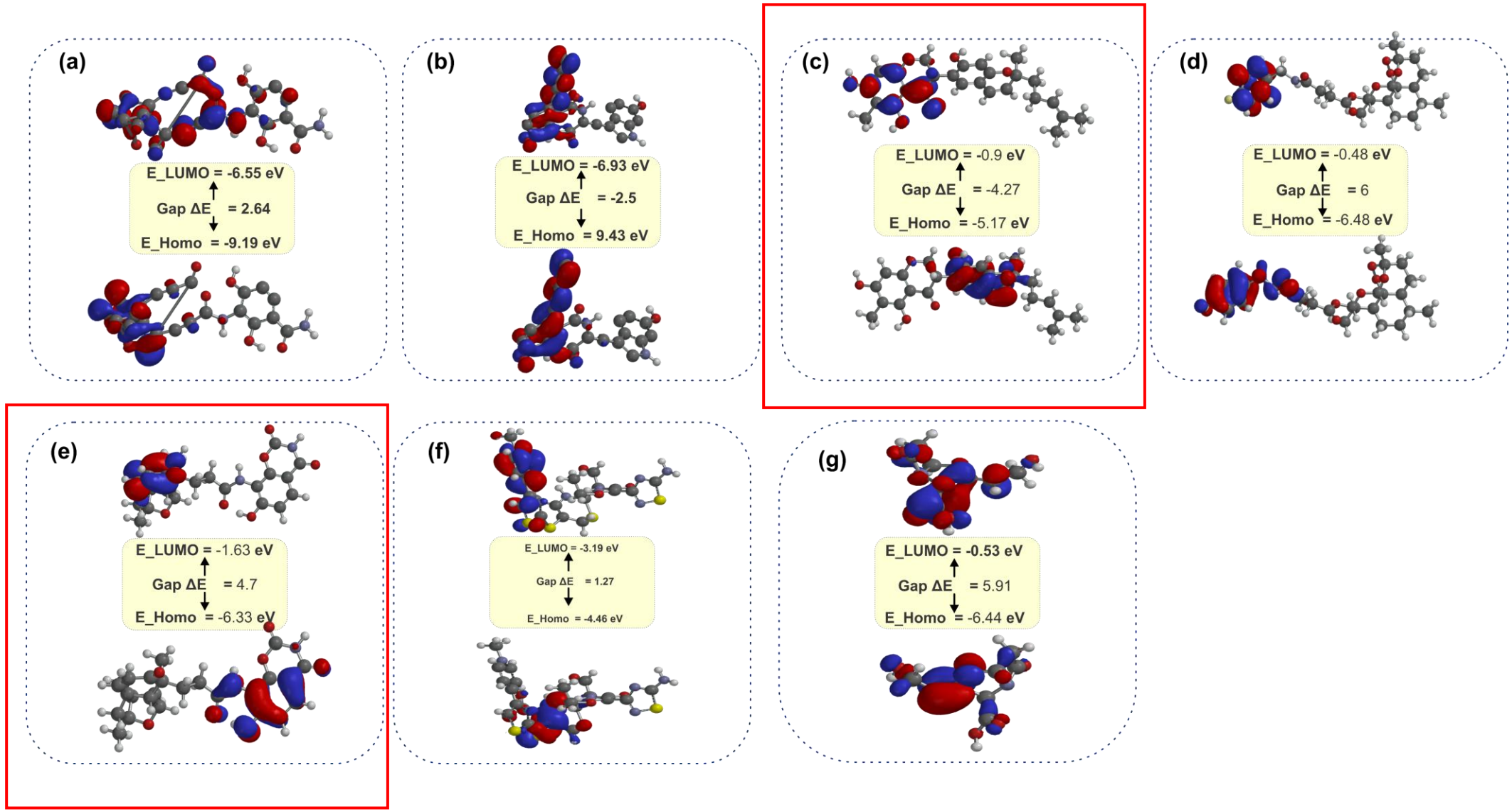


Figure 24: Transition energies of the molecular orbitals for TP64159; (b) TP77265; (c) TP93780; (d) TP124709; (e) TP156670 and (f) ceftaroline (g) clavulanate

**Table 4:** The conceptual density functional theory descriptors of top five terpenoids and reference compounds

| Descriptors (eV) | TP64159 | TP77265 | TP93780 | TP124709 | TP156670 | Ceftaroline | Clavulanate |
|---|---|---|---|---|---|---|---|
| **E_LUMO** | -6.55 | -6.93 | -0.9 | -0.48 | -1.63 | **-3.19** | **-0.53** |
| **E_HOMO** | -9.19 | -9.43 | -5.17 | -6.48 | -6.33 | **-4.46** | **-6.44** |
| **Energy gap (ΔE)** | 2.64 | 2.5 | 4.27 | 6 | 4.7 | **1.27** | **5.91** |
| **Ionization energy** | 9.19 | 9.43 | 5.17 | 6.48 | 6.33 | **4.46** | **6.44** |
| **Electron affinity** | 6.55 | 6.93 | 5.17 | 0.48 | 1.63 | **3.19** | **0.53** |
| **Hardness** | -2.78 | -2.97 | -2.09 | 0.26 | -0.32 | **-1.10** | **0.24** |
| **Softness** | -0.36 | -0.34 | -0.48 | 3.85 | -3.17 | **-0.91** | **4.26** |
| **Electronegativity** | 0.32 | 0.33 | 0.26 | 2.42 | -1.09 | **0.04** | **2.63** |
| **Chemical potential** | -0.32 | -0.33 | -0.26 | -2.42 | 1.09 | **-0.04** | **-2.63** |
| **Electrophilicity index** | -0.14 | -0.16 | -0.07 | 0.76 | -0.19 | **0.00** | **0.81** |

# Conclusion

- Integrated **structure-based pharmacophore** modeling and **molecular docking** identified **five terpenoid leads** with **promising dual inhibitory potential** against *K. pneumoniae* PBP3 and KPC-2 beta-lactamase.

- Selected leads exhibited favourable pharmacokinetics, oral drug-likeness, safe toxicity profiles, and moderate synthetic accessibility, supporting their potential as oral therapeutics.

- TP93780 and TP156670 showed superior negative binding free energies (BFE) compared to reference standards, indicating stronger and more stable interactions.

# Conclusion

- Thermodynamic analysis revealed that these leads relied on a balanced combination of **hydrophobic and moderate electrostatic interactions,** promoting stable binding under physiological conditions.

- Post-MD and PCA and FEL analyses demonstrated **enhanced structural stability**, **more compact conformations, and constrained motions in ligand-bound systems,** supporting functional relevance.

- Overall findings highlight TP93780 (desmodianone A) and TP156670 (platensimycin B2) as robust dual-target candidates, with in vitro studies underway to validate their inhibitory potential.

# Thank you for listening

DUT
DURBAN UNIVERSITY OF TECHNOLOGY
INYUVESI YASETHEKWINI YEZOBUCHWEPHESHE


COMPUTATIONAL & SYSTEMS BIOLOGY RESEARCH GROUP



# Acknowledgement

The NRF is duly acknowledged for providing funding for the study.

The CSBRG with Prof. Sabiu Saheed as lead researcher is acknowledge for the support provided.

The Centre for High-Performance Computing (CHPC), South Africa is equally acknowledged for granting access to the computing systems used in this study.

# Selected references


Alexander, JAN, Worrall, LJ, Hu, J, Vuckovic, M, Satishkumar, N, Poon, R, Sobhanifar, S, Rosell, FI, Jenkins, J & Chiang, D (2023). Structural basis of broad-spectrum β-lactam resistance in Staphylococcus aureus. *Nature,* 613(7943) 375-382.

Kim, C, Milheiriço, C, Gardete, S, Holmes, MA, Holden, MT, de Lencastre, H & Tomasz, A (2012). Properties of a novel PBP2A protein homolog from Staphylococcus aureus strain LGA251 and its contribution to the β-lactam-resistant phenotype. *Journal of Biological Chemistry,* 287(44) 36854-36863.

Linz, MS, Mattappallil, A, Finkel, D & Parker, D (2023). Clinical impact of Staphylococcus aureus skin and soft tissue infections. *Antibiotics,* 12(3) 557.

Mir, MA, Mehraj, U & Sheikh, BA (2021). Recent advances in chemotherapeutic implications of deguelin: a plant-derived retinoid. *The Natural Products Journal,* 11(2) 169-181.

Morris, G. M., Huey, R., Lindstrom, W., Sanner, M. F., Belew, R. K., Goodsell, D. S. & Olson, A. J. (2009). AutoDock4 and AutoDockTools4: Automated docking with selective receptor flexibility. *Journal of computational chemistry,* 30(16) 2785-2791.

O'Boyle, N. (2011). Banck M. James CA Morley C. Vandermeersch T. Hutchison GR Open Babel: An open chemical toolbox. *J. Cheminf,* 3(1) 33.

Trott, O. & Olson, A. J. (2010). AutoDock Vina: improving the speed and accuracy of docking with a new scoring function, efficient optimization, and multithreading. *Journal of computational chemistry,* 31(2) 455-461.